WSRC-TR-2002-00337
Revision 1

KEY WORDS: Performance Assessment
LLW Disposal
Slit Trench
Engineered Trench
Uranium Disposal

SPECIAL ANALYSIS:
Disposal of M-Area Glass in Trenches

Authors

J. R. Cook[a] and A. D. Yu[b]

[a]Westinghouse Savannah River Company
Savannah River Technology Center
Aiken, SC 29808

[b]ALARA Environmental Analysis, Inc

August 21, 2002

Westinghouse Savannah River Company
Savannah River Site
Aiken, SC 29808

REVISION HISTORY

Revision 1 of the document was prepared to address comments derived from the design check process and review by DOE-SW.

EXECUTIVE SUMMARY

The effect of disposing of low-level waste consisting of vitrified sludge from M-Area in slit trenches is evaluated. The conclusion of the analysis is that this waste can be disposed of at SRS and meet the performance objectives of DOE Order 435.1. A comparison of the uranium inventory in the waste and the calculated disposal limits is given in Table ES-1.

Table ES-1. Comparison of the calculated inventory limits for five Slit Trenches or one Engineered Trench and the projected inventory.

Radionuclide	Inventory Limit Ci	Actual Inventory Ci	Limit/Actual Inventory
U-234	4.9E+01	2.8E+00	1.8E+01
U-235	3.7E+01	1.9E-01	2.0E+02
U-236	4.6E+03	1.4E-01	3.3E+04
U-238	2.0E+02	1.1E+01	1.8E+01

INTRODUCTION

M-Area waste sludge accumulated at SRS as a result of plating line, metal-finishing and aluminum-forming operations used to produce nickel-plated, aluminum-clad depleted uranium targets for ^{239}Pu production. The sludge was classified as an F006-listed mixed waste with nickel the primary hazardous constituent and depleted uranium the major radioactive component.

M-Area waste is subject to the land disposal restrictions treatment criteria that require permanent stabilization of F006 wastewater treatment sludges in solid form prior to disposal. A central objective in evaluating treatment technologies is the potential for delisting the hazardous component of the final waste form through submission and approval of a delisting petition. Such a petition has been submitted to and approved by the EPA for the M-Area waste based on the vitrification process and the expected durability of the final waste form.

On March 15, 2002, the EPA published in the Federal Register[1] a proposal to grant the delisting petition for the M-Area waste. Final approval was published in the Federal Register on August 21, 2002[2]. As a result of approval of the delisting petition by the EPA, the M-Area waste can be disposed as low-level waste rather than mixed waste. This Special Analysis provides reasonable assurance that disposal of this waste form will meet the performance objectives of DOE Order 435.1 for low-level waste disposal.

The inventory of each uranium isotope in the M-Area glass and the corresponding trench disposal limit for normal waste forms are shown in Table 1. The amount of ^{238}U exceeds the PA disposal limit. Therefore, a revised set of limits was developed specifically for the vitrified M-Area waste, which took credit for the low leachability of the waste form. That process is documented in this report.

Table 1 Comparison of M-Area Glass inventory and trench disposal limits for unenhanced waste forms

Radionuclide	Inventory in Glass, Ci[3]	Trench Disposal Limit, Ci/5 trenches or 1 ET[4]
U-234	2.8E+00	1.1E+01
U-235	1.9E-01	8.0E+00
U-236	1.4E-01	2.0E+00
U-238	1.1E+01	7.4E+00

Note: Reference 3 includes inventories for Th-234 and Pa-234m. These short-lived daughters are explicitly included in the analysis through decay of the parent U-238.

Glass Dissolution Rate and Contaminant Leach Rate

The mathematical model for glass dissolution and dissolution rates for various glass formulations are described in Whited et al.[5] This paper summarizes the long-term dissolution rates for 13 glass formulations and developed mathematical models using a sound dissolution mechanism. In this section, we will verify the mathematical model and calculate the glass dissolution rate for the M-Area vitrified waste at 25°C. We will also calculate the leach rates of uranium isotopes and daughters assuming simultaneous dissolution and radioactive decay.

Mathematical Model Used for the Dissolution of Glass

In order to verify the mathematical model, we have obtained an analytical solution to the problem that appears on page 307 of Whited et al.[5] The following is the equation derivation based on the "normalized leach rate" concept describing the glass bulk dissolution rate as:

$$-\frac{dm}{Vdt} = k\frac{A_s}{V} \tag{1}$$

where m is the mass (grams) of vitrified glass, V is volume (cm^3), t is time (years), k is normalized dissolution rate (g/cm^2-yr) and A_s is surface area (cm^2). Assume glass is in the shape of a perfect sphere of uniform density ρ (g/cm^3), then

$$m = \rho V \tag{2}$$

$$A_s = 4\pi r^2 \tag{3}$$

$$V = 4\pi r^3 / 3 \tag{4}$$

Substituting equations (2), (3), and (4) into (1) and integrating, we obtain:

$$\int_{R_0}^{r} -dr = \int_{0}^{t} \frac{k}{\rho} dt \tag{5}$$

where R_0 is the initial radius of the sphere. Integrating equation (5) yields

$$r = R_0 - \frac{kt}{\rho} \tag{6}$$

The parameters used for the hypothetical problem in page 307 of Whited et al.[5], are R_o = 1.0 cm, k = 1.0×10^{-3} g/m^2-d = 3.65×10^{-5} g/cm^2-yr, and ρ = 2.6 g/cm^3.

The time for total dissolution of glass (t_x) is obtained by setting $r = 0$ in equation (6), yielding

$$t_x = R_0 \rho / k = 7.12\times10^4 \text{ years.}$$

Based on Equation (1), the dissolution rate (*-dm/dt*) is:

$$-\frac{dm}{dt} = kA_s = 4\pi r^2 k = 4\pi k (R_0 - kt/\rho)^2 \tag{7}$$

The dissolution rate as a function of time calculated by equation (7) is shown in Figure 1. The initial dissolution rate can be calculated as:

$$-\left.\frac{dm}{dt}\right|_{t=0} = 4\pi k R_0^{\,2} = 4.59\times10^{-4} \text{ g/yr.}$$

The above calculations benchmarked published data. The next step is to obtain normalized dissolution rate for M-Area vitrified waste.

M-Area Glass Dissolution Rate

The M-Area vitrified waste is in small pieces of ovoid. Each ovoid has the shape of a hemisphere. Diameter of each hemisphere is 13 mm, or radius = 0.65 cm. Surface to volume ratio is:

$$\frac{A_s}{V} = \frac{3\pi r^2}{2\pi r^3/3} = \frac{4.5}{r} = 6.92 \text{ cm}^{-1} = 692 \text{ m}^{-1}$$

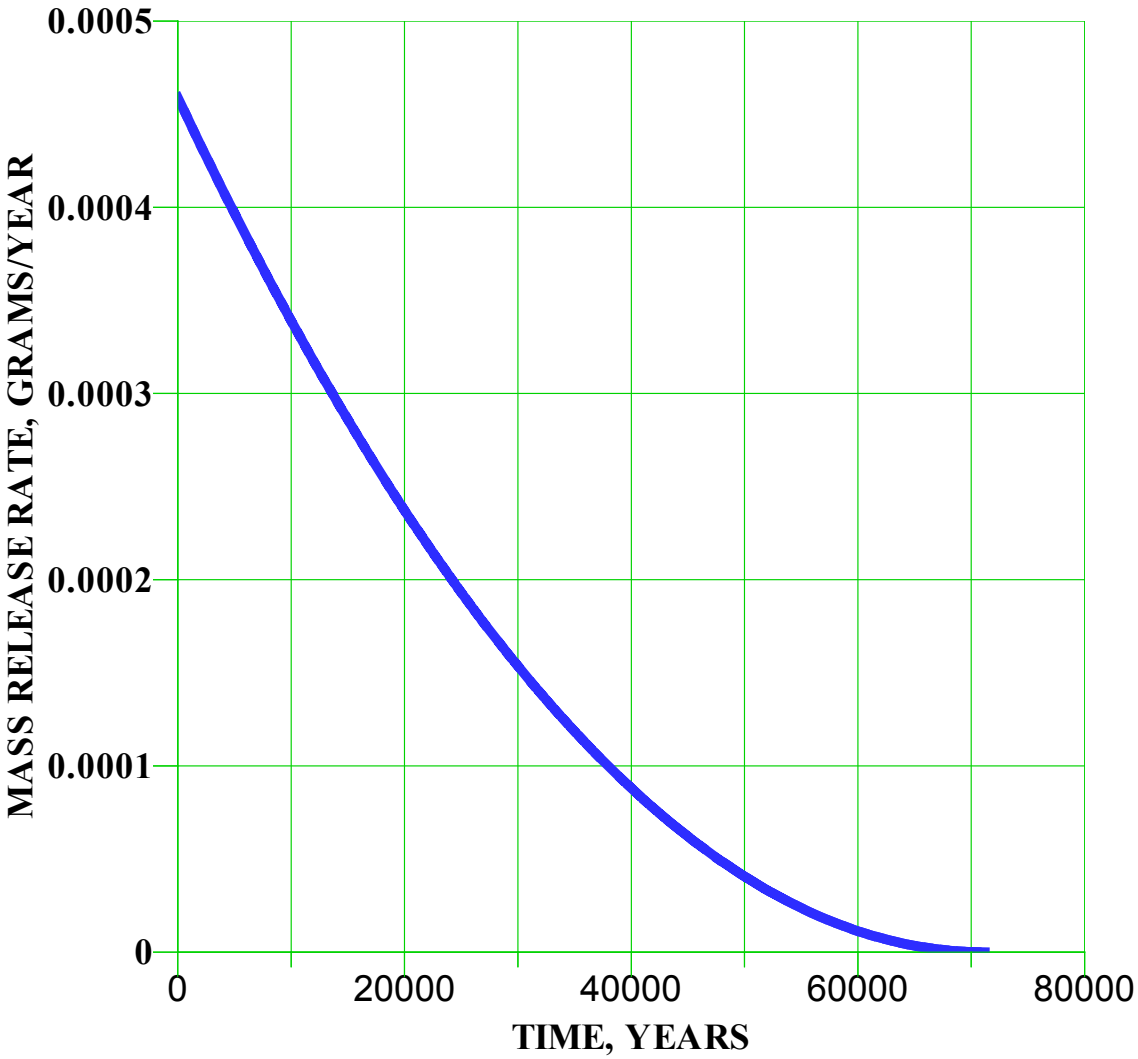

Figure 1. Mass dissolution rate of a hypothetical glass sphere, initial radius = 1.0 cm, normalized dissolution rate = 1.0×10^{-3} g/m^2-d.

Whited et al.[5] summarized the average long-term normalized glass dissolution rate constants for 13 glass formulations and 29 samples in a variety of water types, including some prepared at the Savannah River Technology Center (SRTC). The results for the dissolution rates at 90°C for SRTC-prepared samples of borosilicate glass leached in water from Yucca Mountain pre-reacted with pulverized tuff are shown in Table 2.

Table 2. Long-term dissolution rates of glass samples measured at SRTC.

GLASS	A_s/V (m^{-1})	k ($g/m^2/d$)
SRL-165/42	340	2.3×10^{-4}
	2000	3.1×10^{-4}
SRL-202A	2000	1.2×10^{-3}
	20000	3.2×10^{-2}
SRL-131/11	340	3.9×10^{-3}
	2000	1.1×10^{-3}
SRL-200	340	5.3×10^{-3}
	2000	6.2×10^{-3}
SRL-131A	2000	1.9×10^{-2}
	20000	3.7×10^{-2}

The above long-term dissolution rates are measured at 90°C. They need to be converted to 25°C, the temperature at the slit trenches. The dependence of k on temperature is expressed in an Arrhenius equation:

$$k = A\exp\left(-\frac{E_A}{RT}\right) \tag{8}$$

where A is a constant, E_A is the activation energy, R is the Gas law constant, and T is the absolute temperature. To calculate k at T_2 from k at T_1, the constant A cancels out. Literature values for E_A are between 60,000 and 90,000 Joule/mole. Substituting E_A = 75,000 Joule/mole and R = 8.314 Joule/mole-°K, T_1 = 363°K, and T_2 = 298°K into equation (8), we obtain $k_{298}/k_{363} = 0.0044$. The dissolution rates for all 29 samples, after this temperature correction, is plotted as a cumulative probability function in Figure 2.

Figure 2 is in agreement with Figure 6 of Whited et al.[5] The red circles are the glass samples shown in Table 2. Based on the experimental data, we selected $k = 2.5\times10^{-5}$ g/m^2-d for use in the analysis. This is slightly higher than the value for 50 percent cumulative probability of 1.7×10^{-5} g/m^2-d.

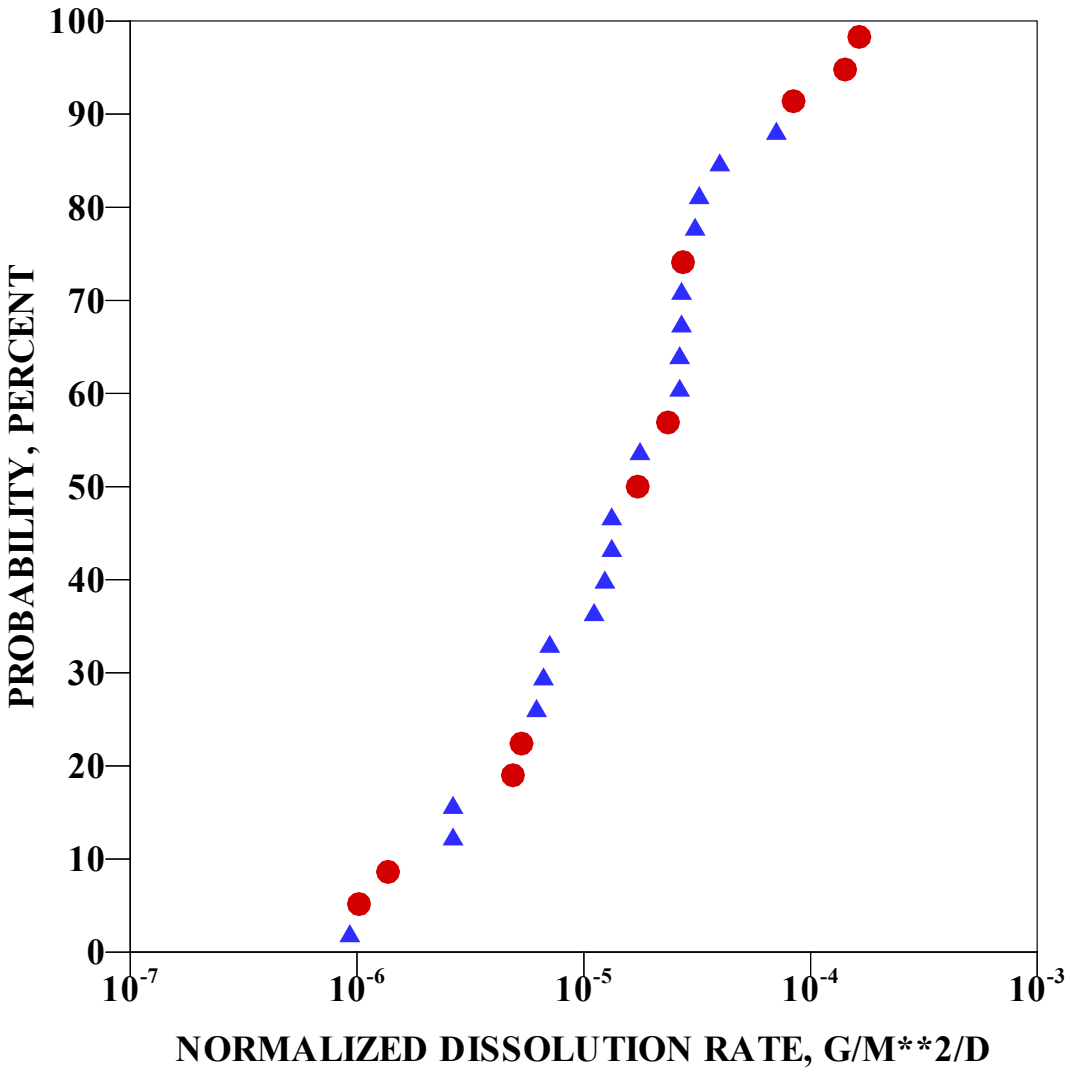

Figure 2. Cumulative probability plot for long-term leach rates at 25°C.

Instead of the mass dissolution rate (in g/year), we are more interested in the fractional dissolution rate, which is the mass rate divided by the initial mass of the ovoid *M*. For a hemisphere

$$M_0 = \rho V_0 = 2\pi R_0^{\,3}\rho/3 \tag{9}$$

When equation (1) for a hemisphere is solved using $A_s=3\pi r^2$ and $V=2\pi r^3/3$, we obtain:

$$r = R_0 - \frac{3kt}{2\rho} \tag{10}$$

The fractional dissolution rate is calculated following the same procedure used to calculate dissolution of a sphere and dividing the dissolution rate by M_o from equation (9). The result is depicted in Figure 3. The cumulative dissolution is also shown. As expected, when the rate diminishes, the cumulative fraction approaches 1.0 at 1.23×10^6 years. The initial fractional dissolution rate is 2.43×10^{-6} year^{-1}. This is in reasonable agreement with the Multiple Extraction Procedure results reported in the Delisting Petition[1] of an equivalent of 0.7% leached over 1,000 years, or 7 x 10^{-6} year^{-1}.

For groundwater compliance, we are only interested in the first 10,000 years. The fractional and cumulative dissolution rates for this time period are shown in Figure 4. The total amount of glass dissolution is about 2.5% after 10,000 years.

Contaminant Leaching from M-Area Vitrified Waste

The focus of this study is on uranium leaching from the waste form to the soil matrix in earthen trenches. We assume the leach rate depends only on glass dissolution and radioactive decay. This assumption accounts for the dominant mechanisms governing contaminant release. The formation of decay daughter(s) and their subsequent release are also modeled.

The vitrified waste is in small pieces of ovoid. Each ovoid has the shape of a hemisphere. Diameter of the hemisphere is 13 mm, or radius = 0.65 cm. We assume that uranium is uniformly distributed in an ovoid so that the leach rate is proportional to the dissolution rate. Mass balance of an isotope *i* in the glass is:

$$\frac{dn_i}{dt} = \delta_{i-1}n_{i-1} - \delta_i n_i + \frac{n_i dV}{Vdt} \tag{11}$$

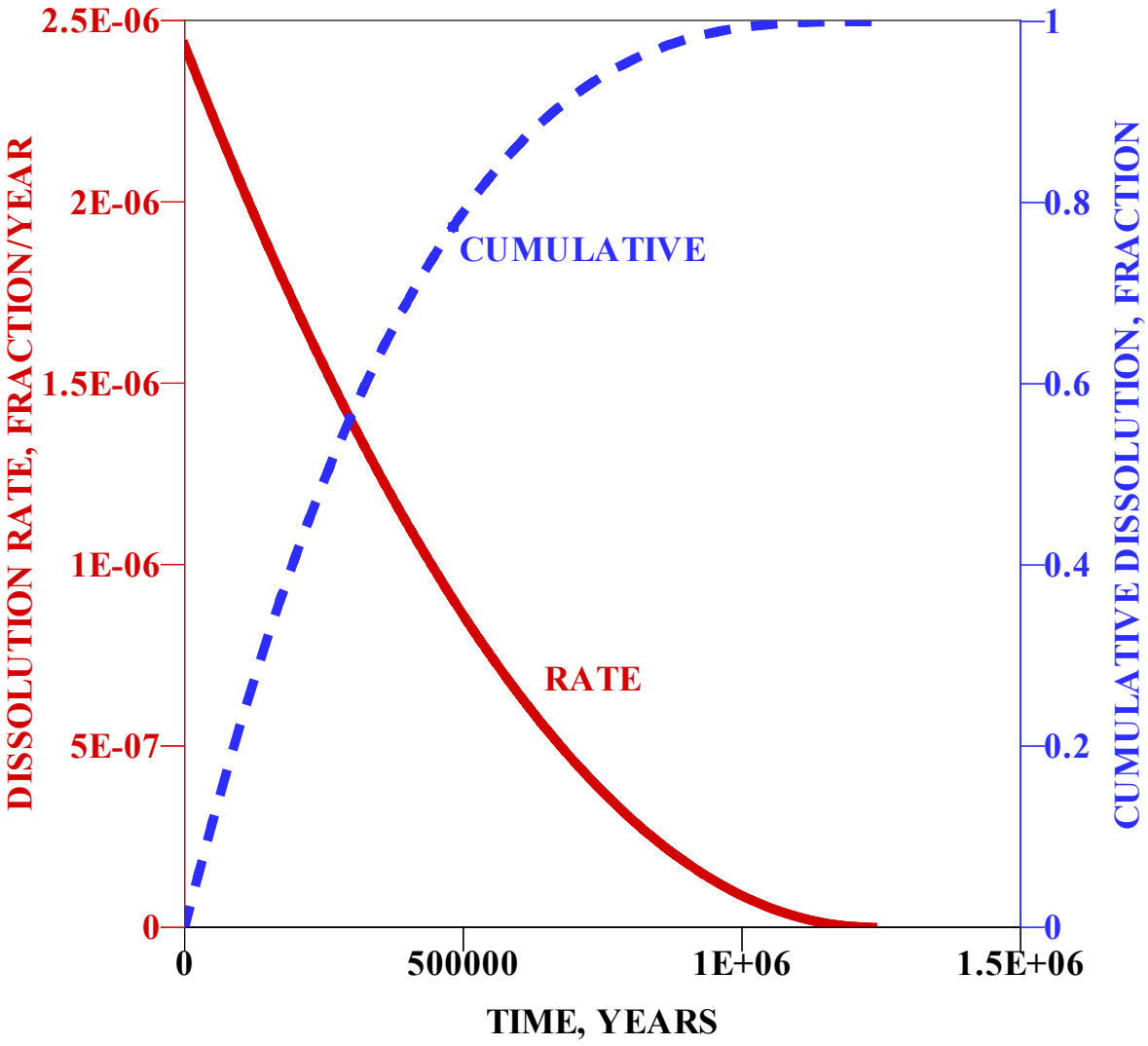

Figure 3. Fractional dissolution rate and cumulative dissolution for M-Area glass, initial radius = 0.65 cm, normalized dissolution rate = 2.5×10^{-5} g/m^2-d at 25^{o}C.

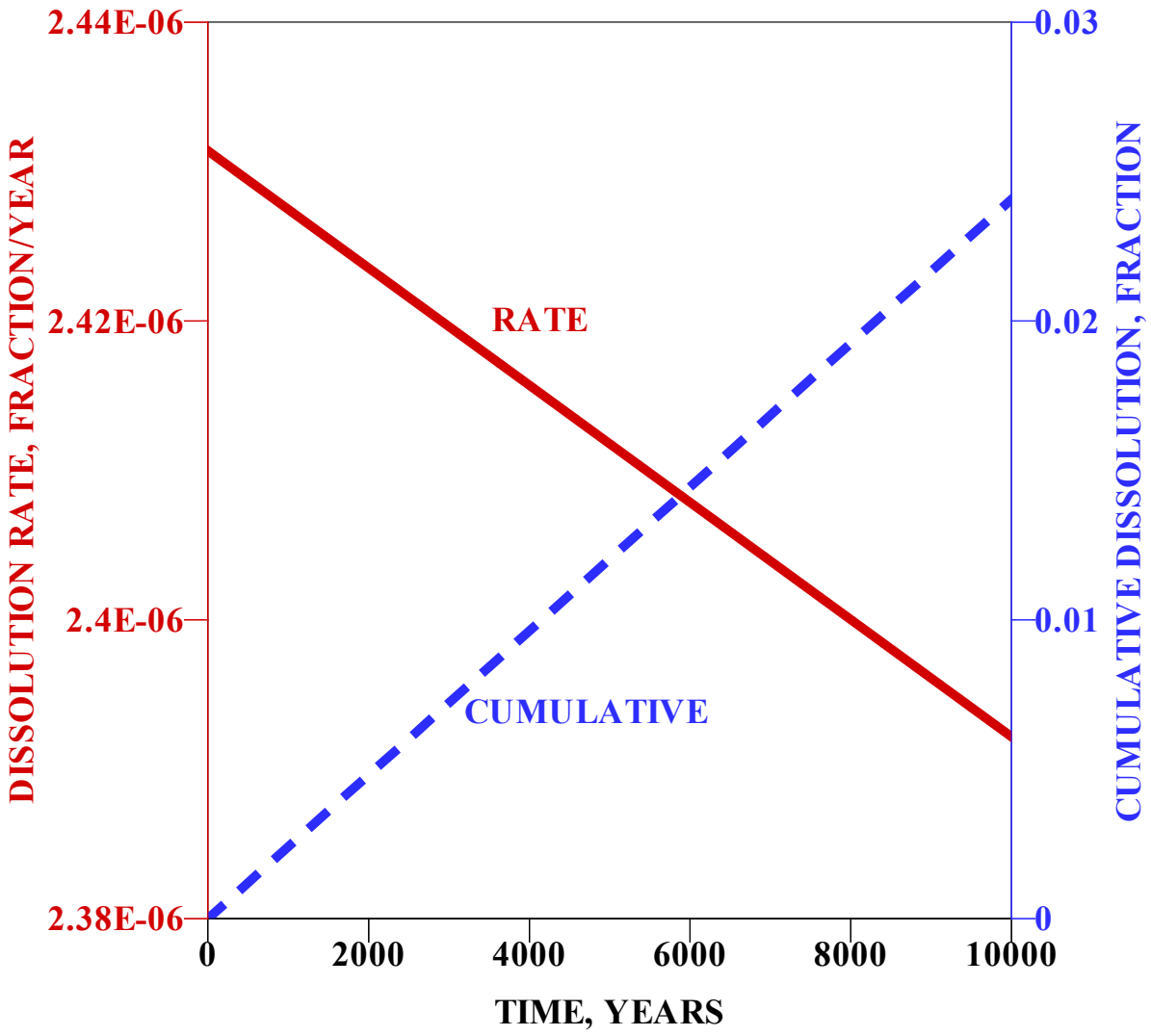

Figure 4. Fractional dissolution rate and cumulative dissolution for M-Area glass in the first 10,000 years.

where n_i is the number of moles of component i in glass, δ is the first-order radioactive decay rate constant, V is the volume of a hemisphere, and i-1 denotes parent of i. We use number of moles for the calculation so that the total moles remaining in glass plus total moles released, summed over all components, is equal to the initial moles of the parent component in glass. The decay rate constant is equated to half-life by:

$$\delta_i = \ln(2) / t_{1/2} \tag{12}$$

where $t_{1/2}$ is the half life of i. For a hemisphere, $V = 2\pi r^3/3$, $A_s = 3\pi r^2$, we obtain:

$$\frac{n_i dV}{Vdt} = \frac{n_i dm}{\rho V dt} = -\frac{n_i k A_s}{\rho V} = -\frac{9 n_i k}{2\rho r} \tag{13}$$

It should be noted that $n_i dV/Vdt$ is always negative because $dV < 0$ at increasing dt. Also, dn_i is always negative for the parent component. However, it can be positive for a daughter isotope. The quantity $-dn_i/dt$ calculated by equation (11) is the fractional leach rate for component i.

To calculate the leach rate, we start with $n_1 = 1.0$ mole at $t = 0$ for the parent component. For each daughter, the initial quantity is set to 0. At a given time t, dn_i/dt can be calculated by the right hand side of equation (11). If we multiply it by a very small time increment dt to obtain dn_i, then $n_i + dn_i$ becomes the moles of component i remaining in glass at $t+dt$. In a FORTRAN program, we used a constant $dt = 0.001$ year and performed the iterative calculation until $t >$ 10,000 years.

To validate the program calculations, we have tracked the mass balance for every decay chain using U-238 as an example. The radioactive decay chain is:

$$\text{U238} \rightarrow \text{Th-234} \rightarrow \text{U-234} \rightarrow \text{N}_\text{C}+1$$

where N_C+1 denotes a hypothetical component comprising the immediate decay daughter of U-234 plus all subsequent daughters. For mass balance purposes, we assume N_C+1 does not go through further decay and dissolution. As can be seen in Table 3, this quantity increases monotonously with time. In the computer program, the amount of each component and the amount of the first three components leached are calculated. The sum of columns 2 to 6 is entered in the last column under "Total". Based on 1.00 mole of U-238 initially, every number under "Total" should be 1.00 as indicated in Table 3. Mass is conserved.

Table 3. Mass balance for the U-238 decay/dissolution processes.

Time	Number of moles					
(Years)	U-238	Th-234	U-234	N_C+1	Leached	Total
0.0	1.00E+00	0.00E+00	0.00E+00	0.00E+00	0.00E+00	1.0000
1.4	1.00E+00	1.48E-11	2.04E-10	3.78E-16	3.43E-06	1.0000
2.7	1.00E+00	1.48E-11	4.06E-10	1.50E-15	6.59E-06	1.0000
4.4	1.00E+00	1.48E-11	6.69E-10	4.08E-15	1.07E-05	1.0000
6.5	1.00E+00	1.48E-11	9.95E-10	9.01E-15	1.58E-05	1.0000
9.3	1.00E+00	1.48E-11	1.43E-09	1.86E-14	2.26E-05	1.0000
17.3	1.00E+00	1.48E-11	2.67E-09	6.50E-14	4.21E-05	1.0000
22.8	1.00E+00	1.48E-11	3.52E-09	1.13E-13	5.55E-05	1.0000
29.5	1.00E+00	1.48E-11	4.56E-09	1.90E-13	7.18E-05	1.0000
37.7	1.00E+00	1.48E-11	5.83E-09	3.10E-13	9.17E-05	1.0000
47.6	1.00E+00	1.48E-11	7.37E-09	4.95E-13	1.16E-04	1.0000
59.6	1.00E+00	1.48E-11	9.23E-09	7.77E-13	1.45E-04	1.0000
91.5	1.00E+00	1.48E-11	1.42E-08	1.83E-12	2.23E-04	1.0000
112.5	1.00E+00	1.48E-11	1.74E-08	2.77E-12	2.74E-04	1.0000
137.9	1.00E+00	1.48E-11	2.14E-08	4.16E-12	3.35E-04	1.0000
168.5	1.00E+00	1.48E-11	2.61E-08	6.22E-12	4.10E-04	1.0000
205.2	1.00E+00	1.48E-11	3.18E-08	9.22E-12	4.99E-04	1.0000
249.2	9.99E-01	1.48E-11	3.86E-08	1.36E-11	6.06E-04	1.0000
302.0	9.99E-01	1.48E-11	4.68E-08	2.00E-11	7.34E-04	1.0000
365.2	9.99E-01	1.48E-11	5.65E-08	2.92E-11	8.88E-04	1.0000
531.2	9.99E-01	1.48E-11	8.22E-08	6.18E-11	1.29E-03	1.0000
639.2	9.98E-01	1.47E-11	9.89E-08	8.95E-11	1.55E-03	1.0000
768.1	9.98E-01	1.47E-11	1.19E-07	1.29E-10	1.87E-03	1.0000
921.9	9.98E-01	1.47E-11	1.42E-07	1.86E-10	2.24E-03	1.0000
1105.4	9.97E-01	1.47E-11	1.71E-07	2.67E-10	2.69E-03	1.0000
1324.2	9.97E-01	1.47E-11	2.04E-07	3.83E-10	3.22E-03	1.0000
1585.1	9.96E-01	1.47E-11	2.44E-07	5.49E-10	3.85E-03	1.0000
1896.2	9.95E-01	1.47E-11	2.92E-07	7.85E-10	4.60E-03	1.0000
2267.1	9.95E-01	1.47E-11	3.49E-07	1.12E-09	5.50E-03	1.0000
2709.3	9.93E-01	1.47E-11	4.16E-07	1.60E-09	6.57E-03	1.0000
3236.4	9.92E-01	1.47E-11	4.96E-07	2.28E-09	7.85E-03	1.0000
3864.8	9.91E-01	1.46E-11	5.90E-07	3.24E-09	9.37E-03	1.0000
4222.9	9.90E-01	1.46E-11	6.44E-07	3.87E-09	1.02E-02	1.0000
5040.8	9.88E-01	1.46E-11	7.67E-07	5.50E-09	1.22E-02	1.0000
6015.7	9.85E-01	1.46E-11	9.12E-07	7.82E-09	1.46E-02	1.0000
7177.6	9.83E-01	1.45E-11	1.08E-06	1.11E-08	1.74E-02	1.0000
8562.3	9.79E-01	1.45E-11	1.29E-06	1.57E-08	2.07E-02	1.0000
10212.6	9.75E-01	1.44E-11	1.52E-06	2.23E-08	2.46E-02	1.0000

Calculated Leach Rates

Calculated leach rates for the four uranium isotopes and their daughter(s) are shown in Figures 5 through 8. To facilitate discussion, it is necessary to include the half life of the components as shown in Table 4.

Table 4. Half life of the modeled components.

Component	Half Life, Years[a]
U-234	2.45E+05
Th-230	7.70E+04
Ra-226	1.62E+03
Pb-210	2.23E+01
Po-210	3.79E-01
U-235	7.04E+08
Pa-231	3.28E+04
Ac-227	2.18E+01
Th-227	5.13E-02
Ra-223	3.13E-02
U-236	2.34E+07
U-238	4.47E+09
Th-234	6.60E-02
U-234	2.45E+05

[a] Data from Reference 6

In the decay chain U234 → Th-230 → Ra-226→ Pb-210 → Po-210, the half lives for the five isotopes are in descending order with the first three isotopes being relatively stable. As expected, the fractional leach rates are in the same descending order as shown in Figure 5. The distance between adjacent curves is proportional to the ratio between the half lives.

Figure 6 depicts the fractional leach rates for U235 → Pa-231 → Ac-227→ Th-227 → Ra-223. The half lives are also in descending order. The distance between Th-227 and Ra-223 is small because their half lives are very close.

U-236 has a half life of 2.34E+07 years. Its fractional leach rate is shown in Figure 7.

In the decay chain U238 → Th-234 → U-234, both U-238 and U-234 are relatively long-lived isotopes whereas Th-234 is short-lived. In a 10,000 year time scale, Th-234 essentially decays into U-234 instantaneously. The amount of U-234 increases in the glass, even if it is a relatively small quantity, due to the long half life of U-238. The leach rate of U-234 also increases. Leach rates are shown in Figure 8.

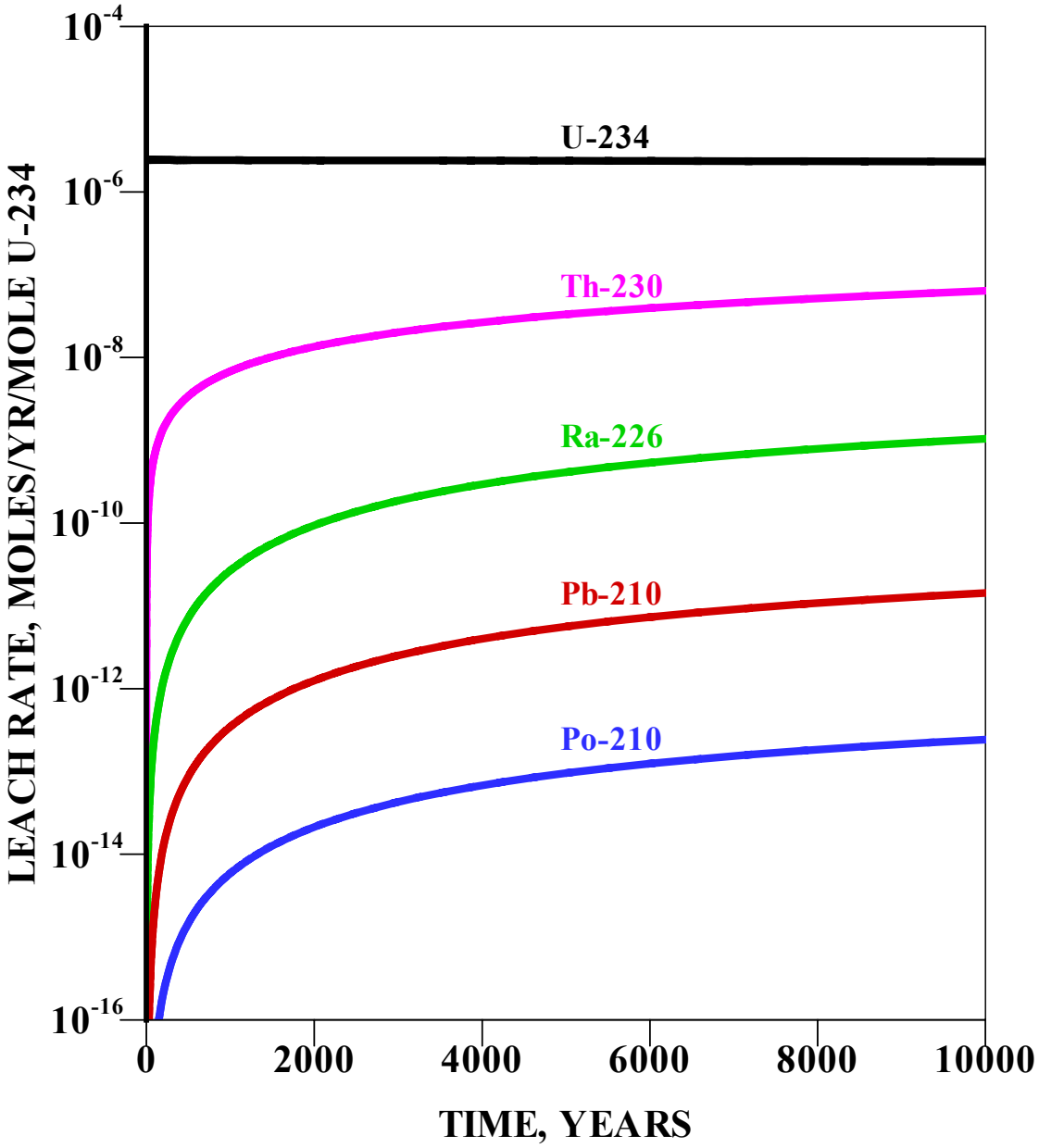

Figure 5. Leach rates for U234 → Th-230 → Ra-226→ Pb-210 → Po-210.

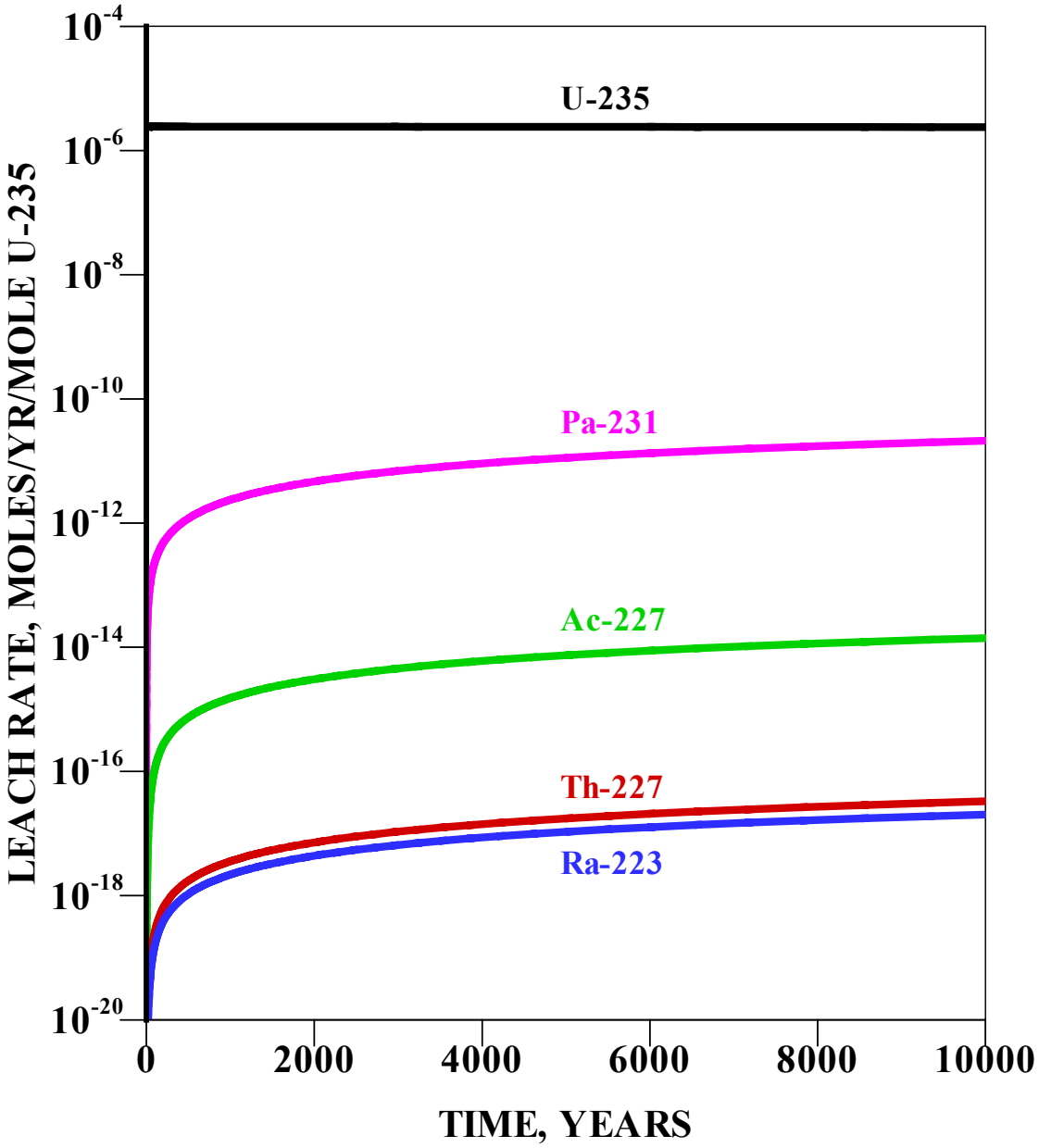

Figure 6. Leach rates for U235 → Pa-231 → Ac-227→ Th-227 → Ra-223.

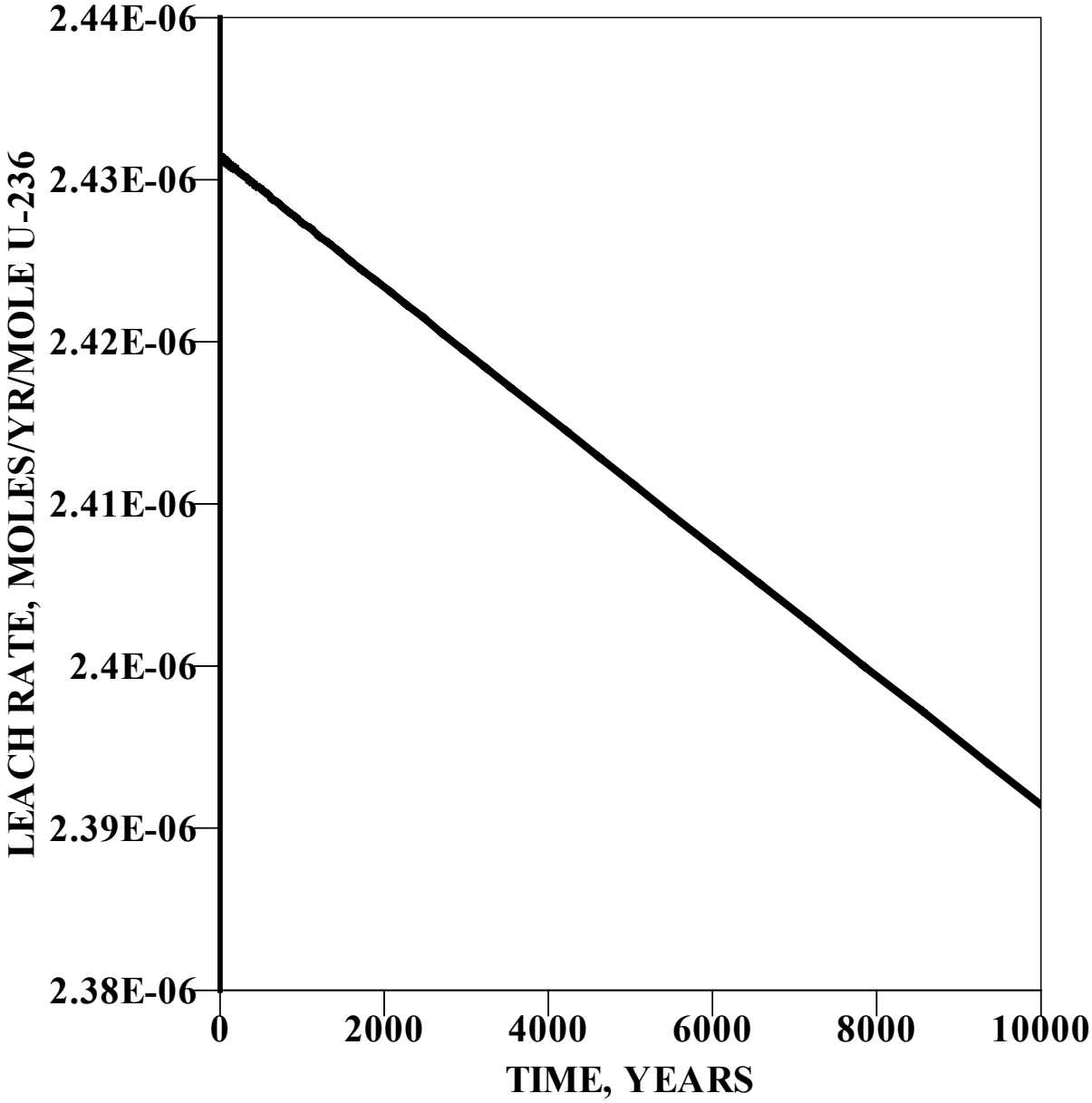

Figure 7. Leach rate for U-236.

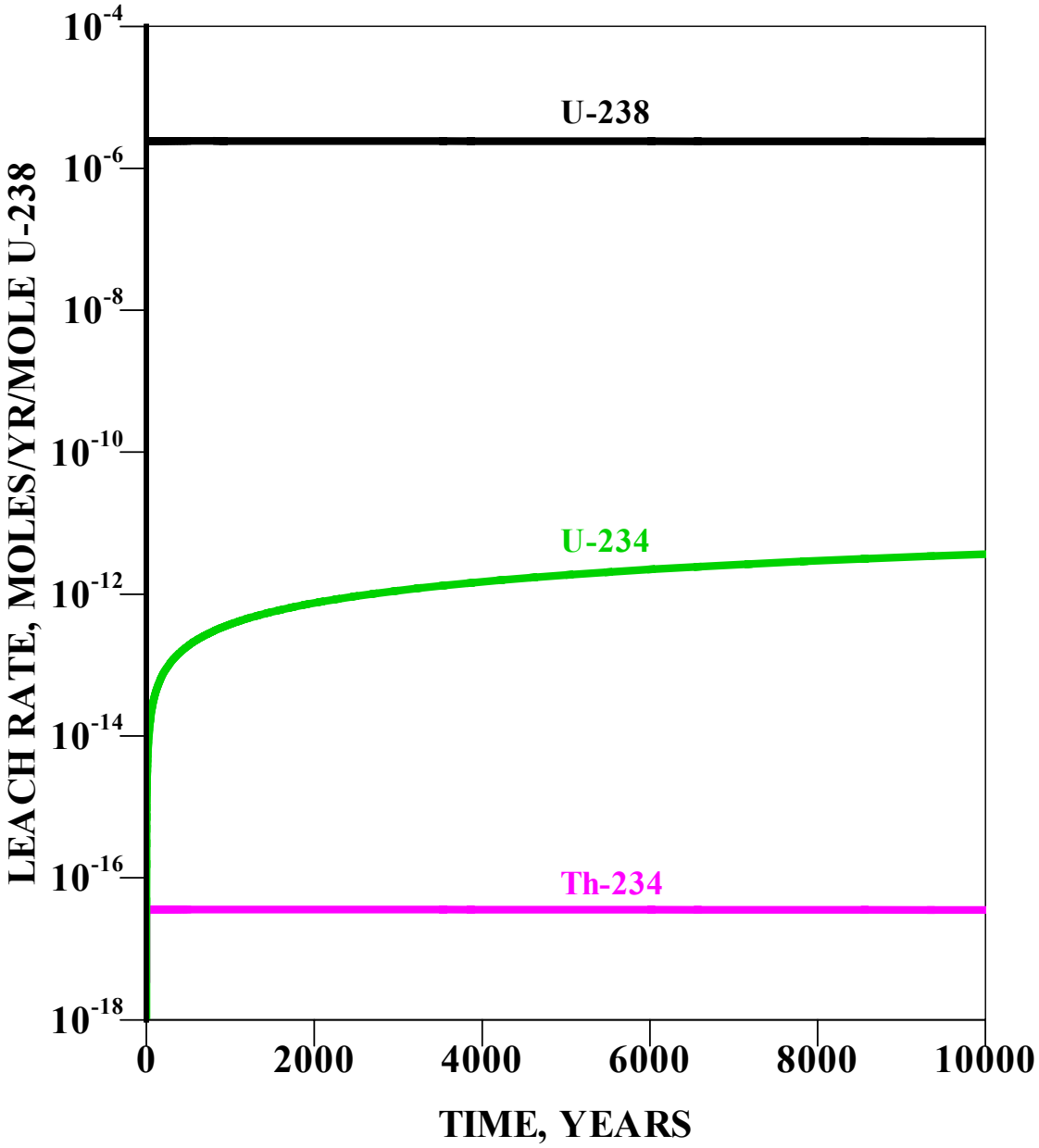

Figure 8. Leach rates for U-238 → Th-234 → U-234.

The fractional leach rate of each isotope is used as a time-dependent source term for the unsaturated-zone transport model using PORFLOW.[7] It is the rate an isotope is released from glass to soil based on 1.0 mole of the parent radionuclide. Once an isotope is in the soil, PORFLOW was used to model the advection, diffusion, adsorption, and decay to simulate contaminant migration to the water table in a flow field represented by the intrinsic properties of the waste disposal facility and the boundary conditions. These are discussed in the following sections.

FLOW AND TRANSPORT MODELING WORK

Conceptual Model

The conceptual model and the two-dimensional model grid used in this study are shown in Figure 9. This shows a single slit trench, twenty feet wide and twenty feet deep, with a fifteen foot thick waste zone and five feet of clean soil over the waste. Over this is a closure cap consisting of backfill, clay, gravel and top soil. Three states of the closure cap were modeled, no cap, intact cap and failed cap. The waste zone was assumed to be a mixture of glass ovoids surrounded by soil. A test case was run with no soil in the waste zone, which produced concentrations about a factor of two higher than for the conceptual model used.

Vadose Zone Flow and Transport

The hydraulic properties for each of the materials in the conceptual model for the no cap, intact cap and failed cap stages are shown in Table 5. The moisture characteristic curves for each of the materials are shown in Figures 10 and 11. The PORFLOW computer program[7] was used to calculate the steady-state flow field for each of the three stages. the velocity and saturation profiles for each stage are shown in Figures 12 through 18. There are two velocity profiles shown for the intact cap stage, one for the cap system and one for the materials under the cap, due to the great difference in the value of the velocity vectors in these areas.

The PORFLOW computer program was also used to calculate the flux of each of the species considered to the water table. The partition coefficient (K_d) for each species in the study is given in Table 6. The results of the vadose zone transport calculations are shown in Figures 19 through 22 and Table 7.

Saturated Zone Flow and Transport

As was done in the PA, the three-dimensional saturated zone flow field was calculated using the FACT computer program with site-specific field data as primary input. Figure 23 shows the horizontal component of flow in the study area. Figure 24 shows the horizontal location of the trench source nodes, representing 2 sets of five trenches, and the nodes representing 100 meter compliance points. The PORFLOW computer program was used to calculate the three dimensional transport of uranium in the saturated zone. Figures 25 through 28 show the concentration in groundwater at the 100-meter well versus time for each of the species considered.

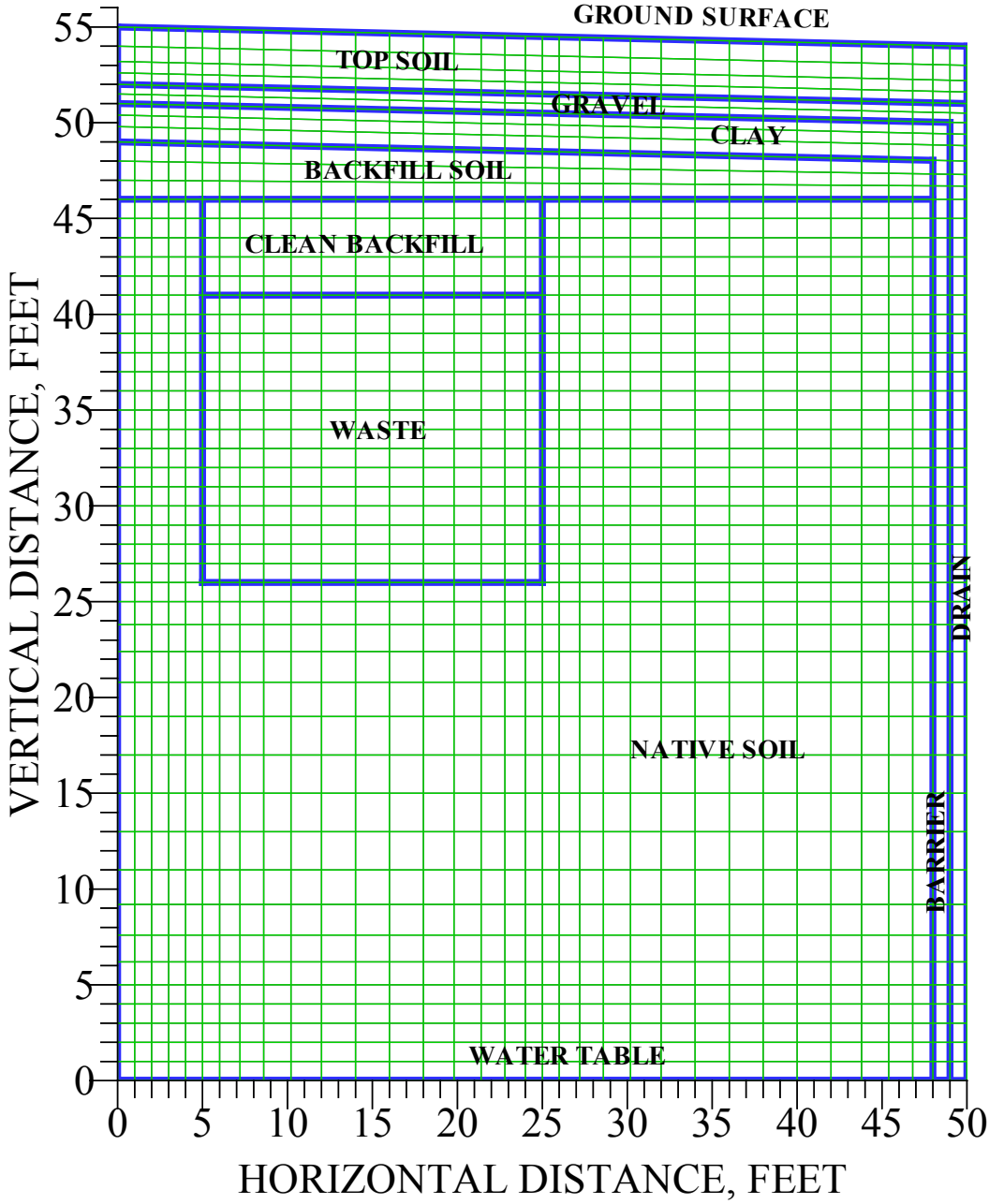

Figure 9. Conceptual model and modeling grid used for the Slit Trench waste disposal.

Table 5. Saturated hydraulic conductivity of and molecular diffusivity in the porous media.

	Hydraulic Conductivity, cm/year			
	No Cap	Intact Cap	Failed Cap	Diffusivity
Porous Media	0-25 years	25-125 years	125-10,000 years	cm^2/year
Native Soil	315.4	315.4	315.4	158
Backfill Soil / Clean Backfill	NA	31.54	31540	158
Waste	315.4	315.4	31,540	158
Top Soil	NA	31540	31,540	158
Gravel	NA	315,400	31,540	158
Clay	NA	3.154	31,540	31.5
Barrier	NA	0.00315	315.4	0
Drain	NA	3,154,000	315.4	0

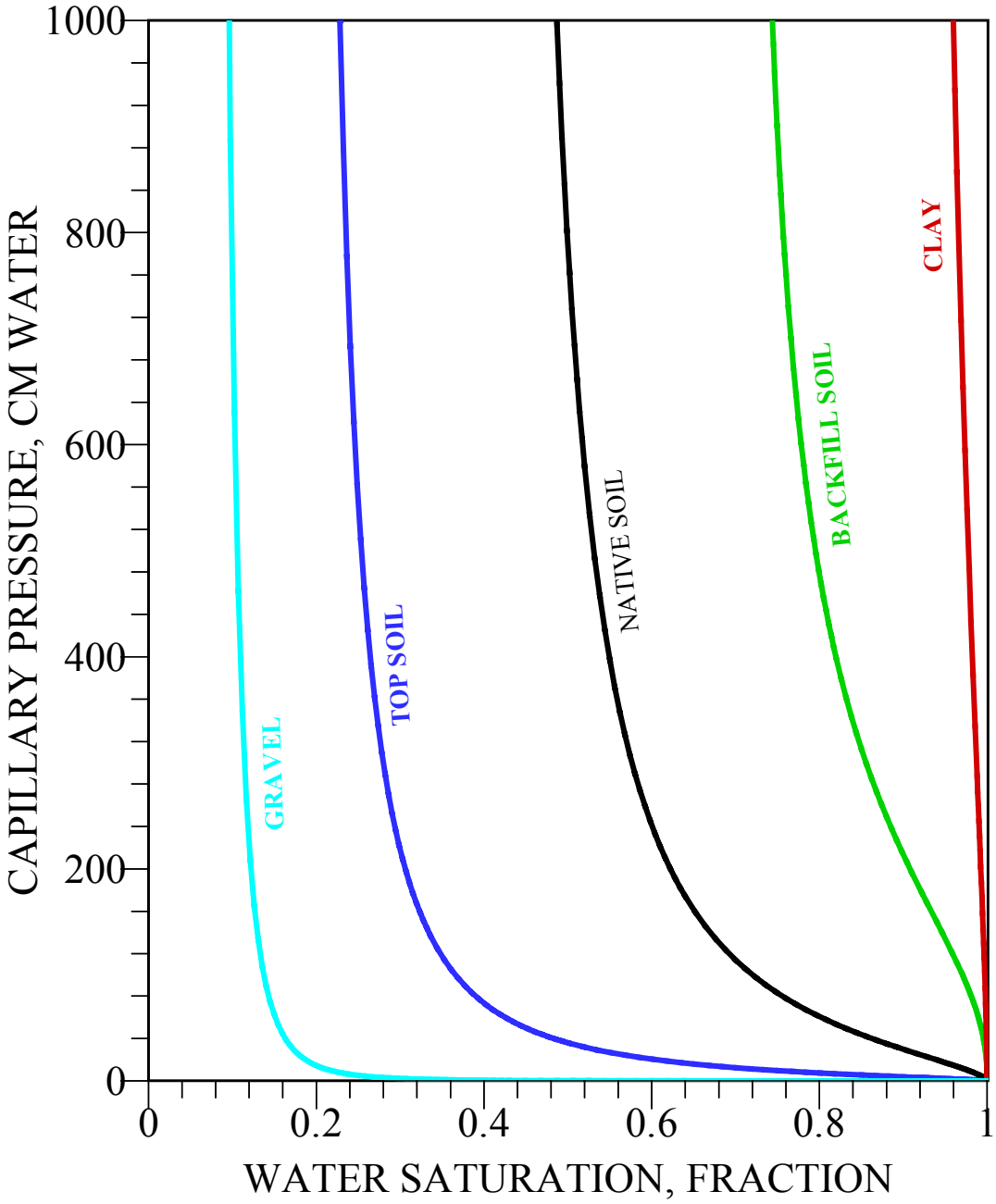

Figure 10. Capillary pressure curves used for the unsaturated-zone modeling.

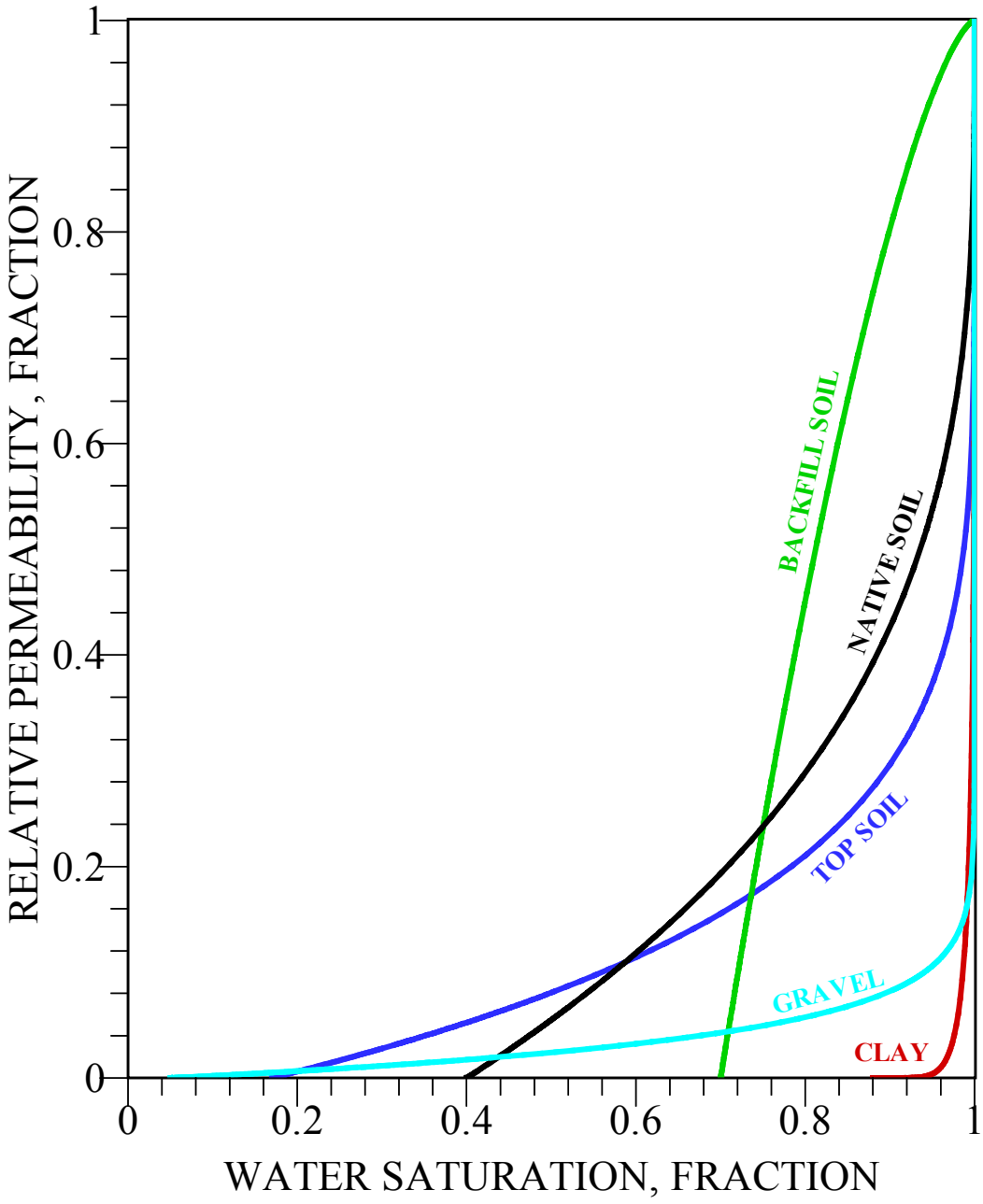

Figure 11. Relative permeability curves used for the unsaturated-zone modeling.

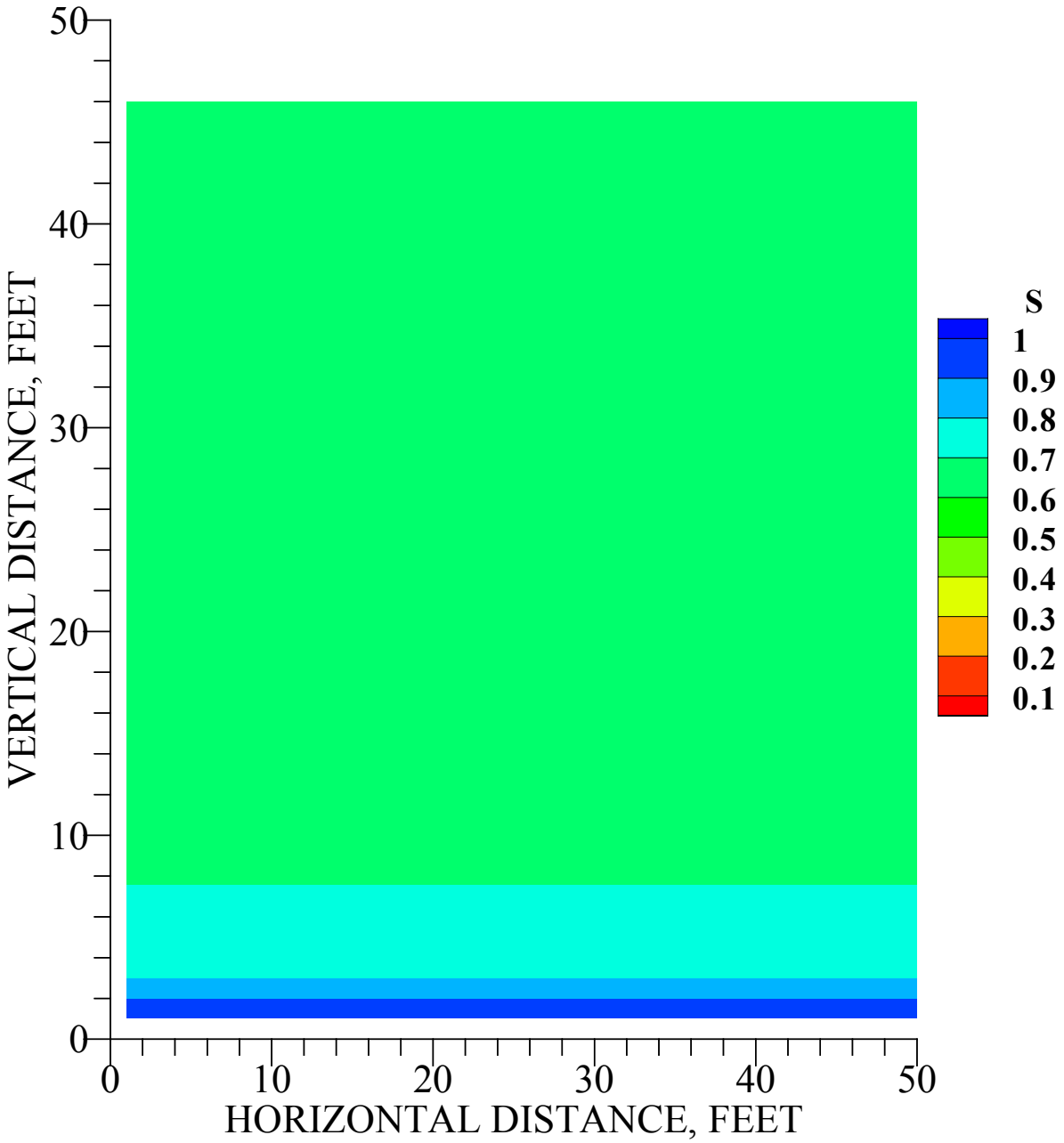

Figure 12. Saturation profile for the No Cap period (0 to 25 years).

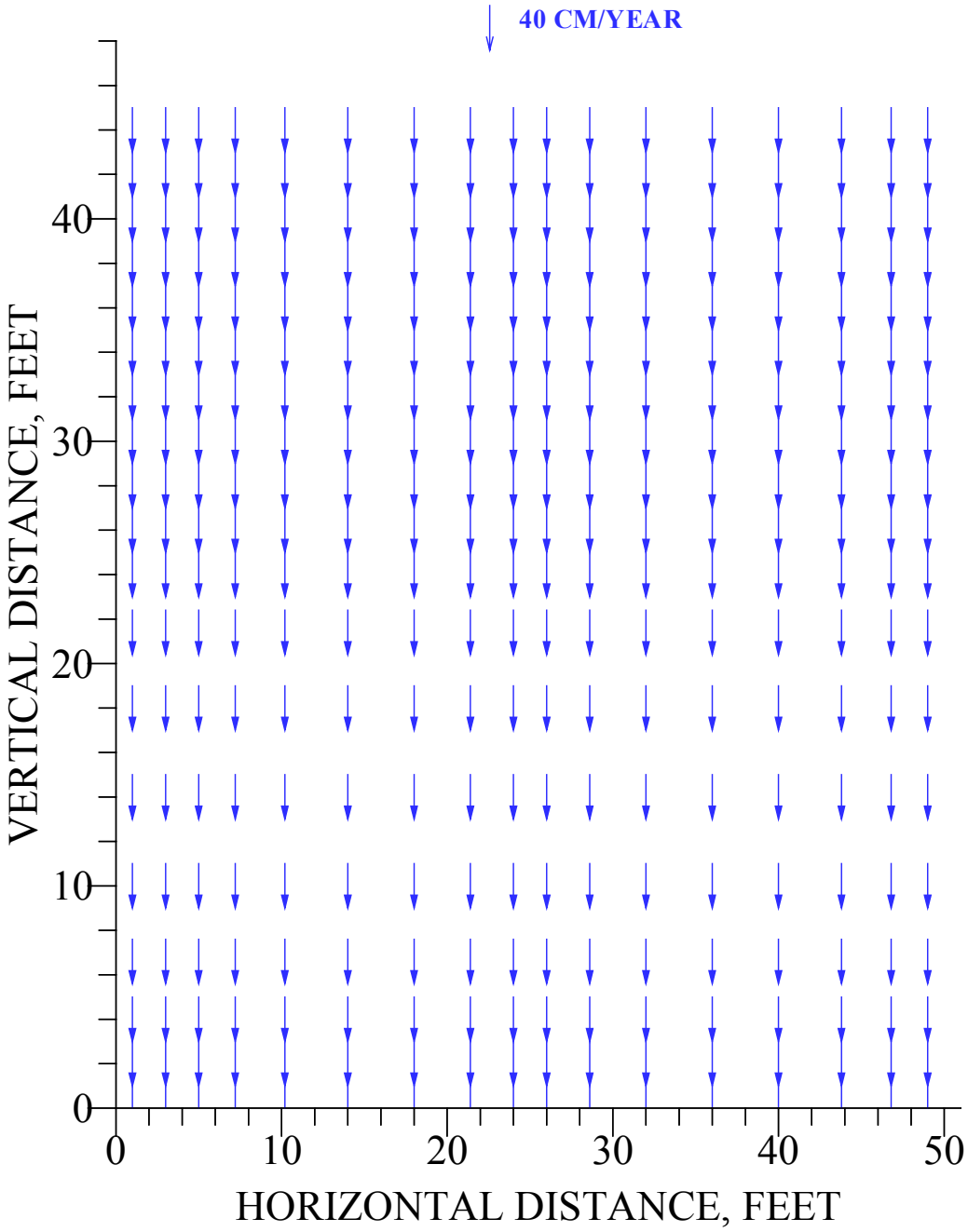

Figure 13. Velocity profile for the No Cap period (0 to 25 years).

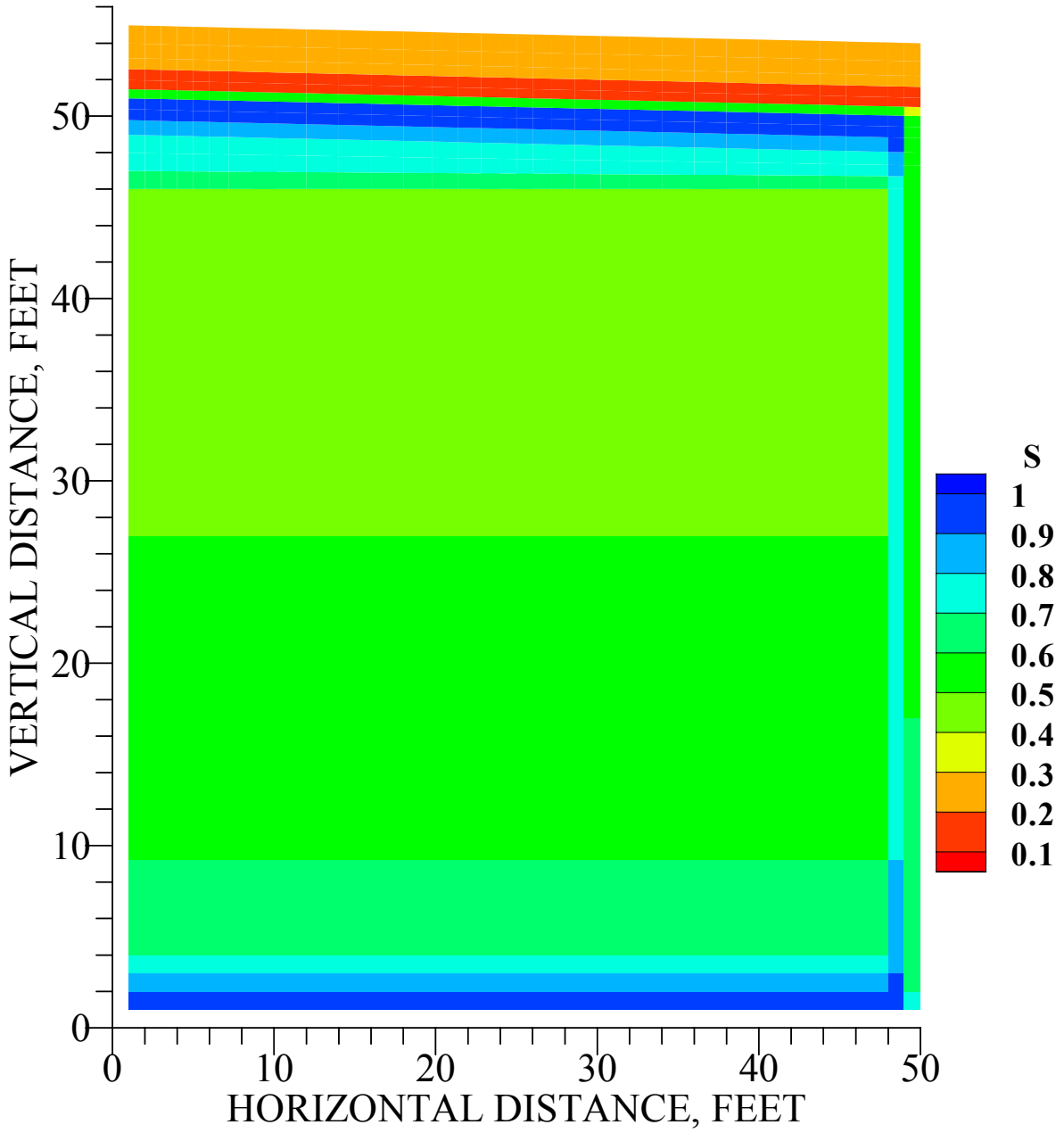

Figure 14. Saturation profile for the Intact Cap period (25 to 125 years).

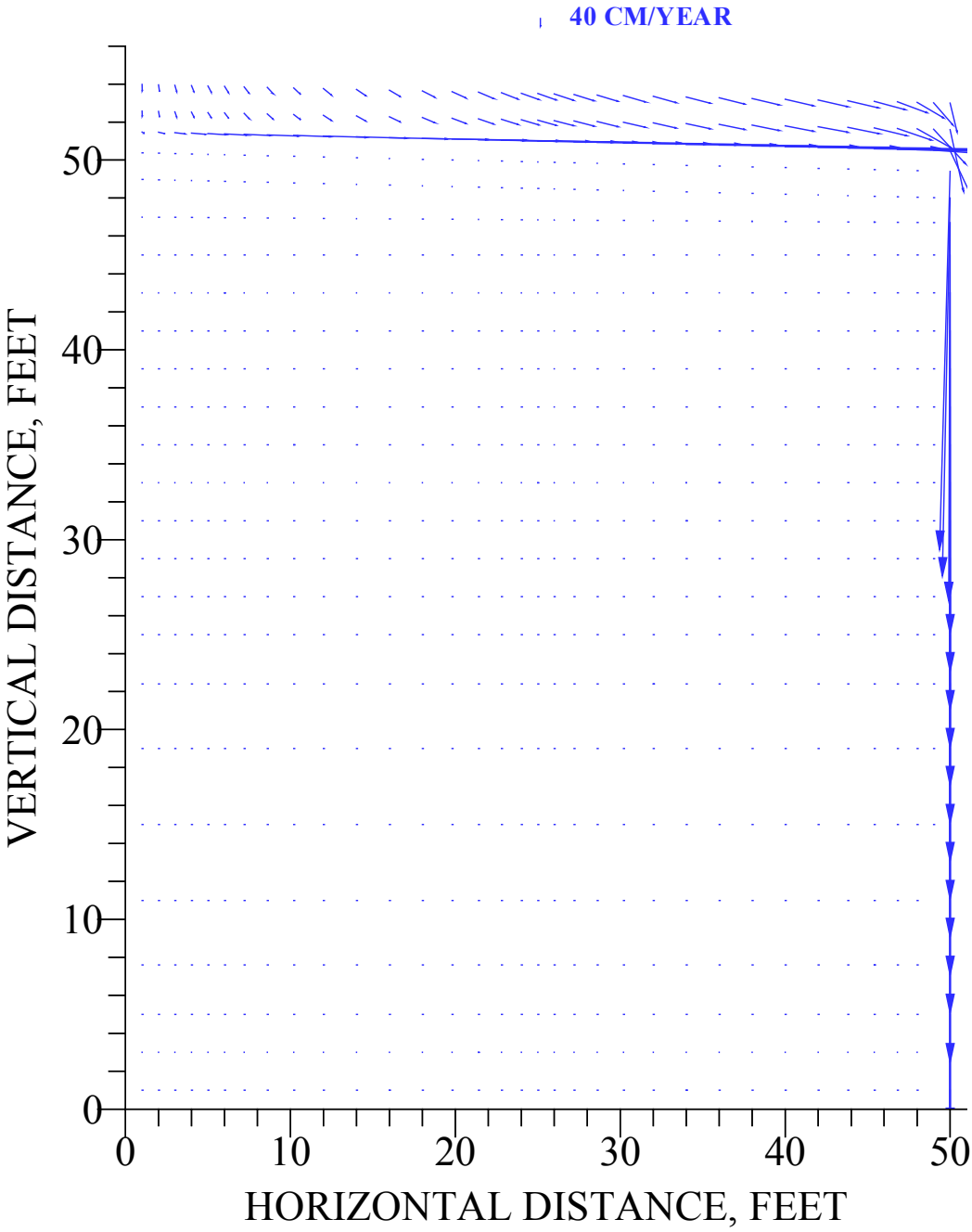

Figure 15. Velocity profile for the Intact Cap period (25 to 125 years).

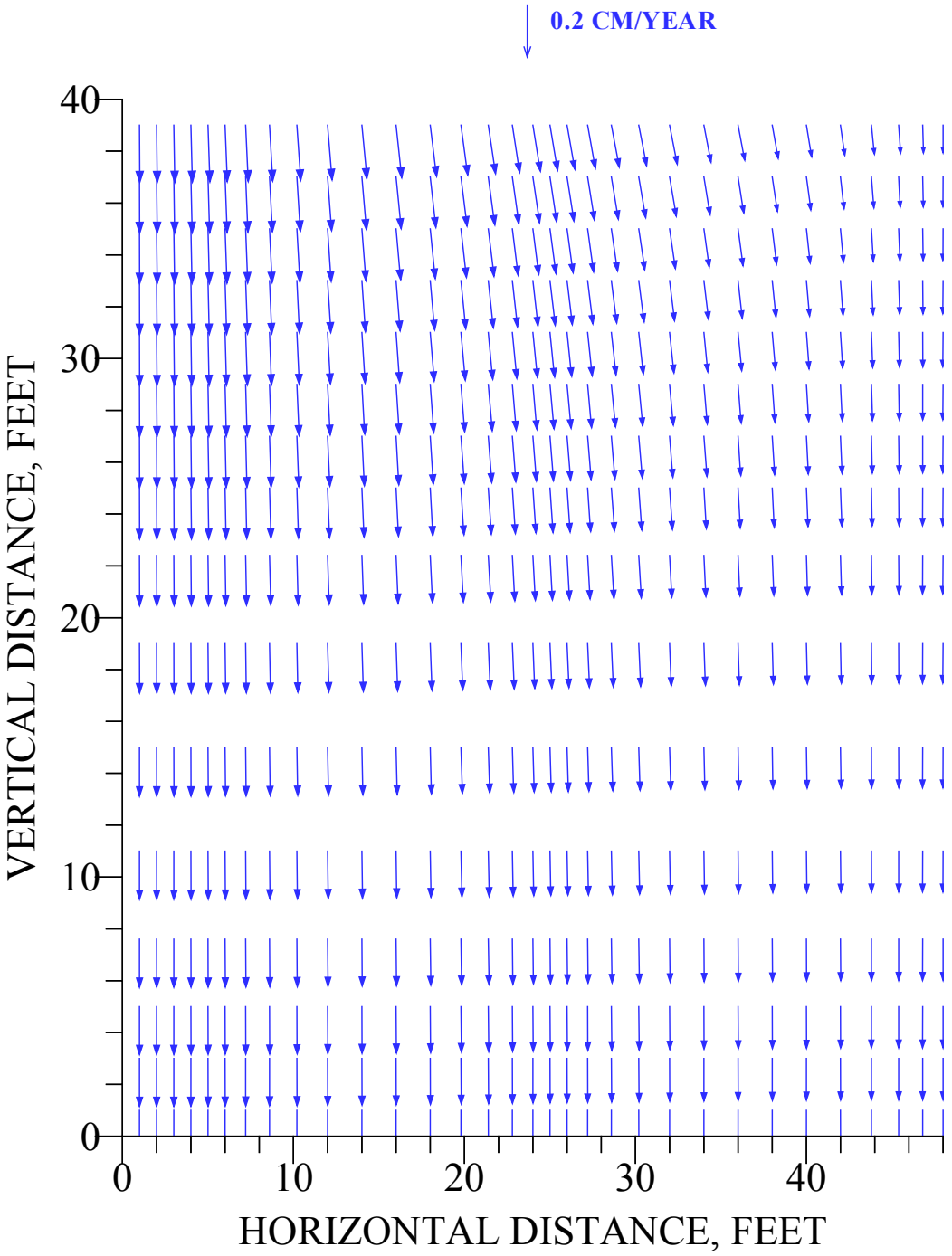

Figure 16. Velocity profile under the cap for the Intact Cap period (25 to 125 years).

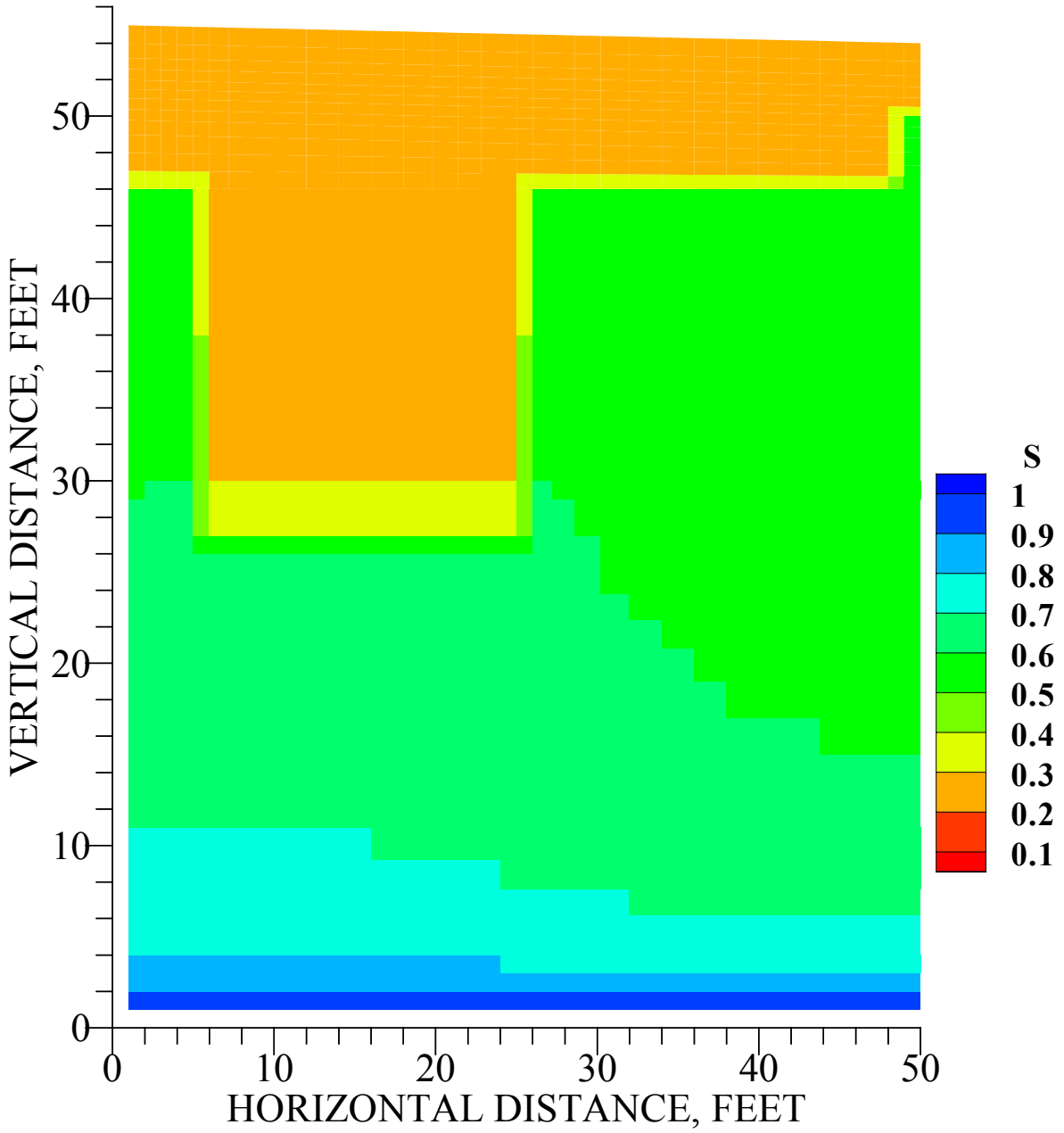

Figure 17. Saturation profile for the Failed Cap period (125 to 10,000 years).

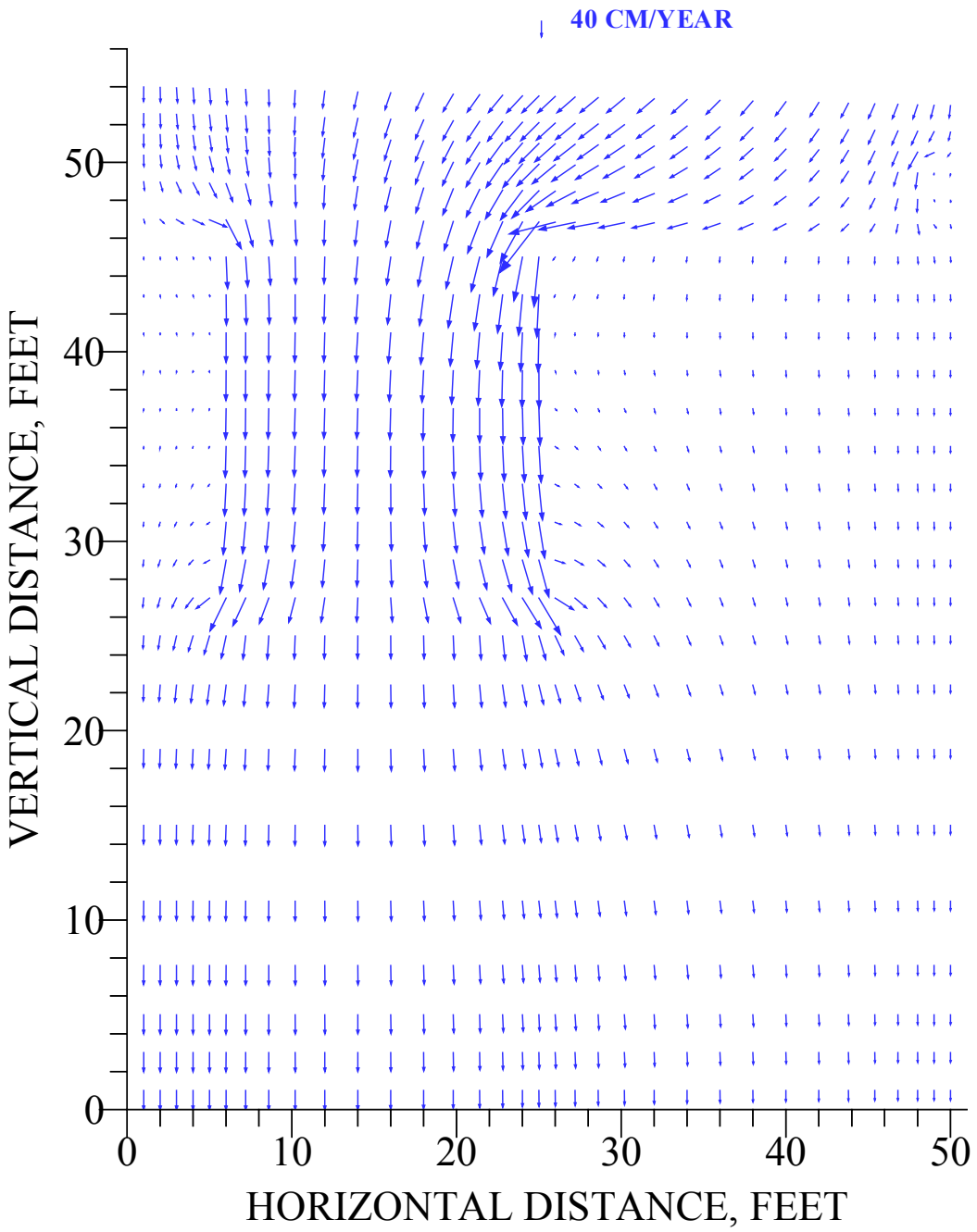

Figure 18. Velocity profile for the Failed Cap period (125 to 10,000 years).

Table 6 Partition Coefficients Used (ml/g)[a]						
Radionuclide	Waste	Backfill and Soil[b]	Gravel	Clay	Barrier[c]	Drain[c]
U-234	800	800	35	1600	800	800
Th-230	3200	3200	3200	5800	3200	3200
Ra-226	500	500	500	9100	500	500
Pb-210	270	270	270	550	270	270
Po-210	150	150	150	3000	150	150
U-235	800	800	35	1600	800	800
Pa-231	550	550	550	2700	550	550
Ac-227	450	450	450	2400	450	450
Th-227	3200	3200	3200	5800	3200	3200
Ra-223	500	500	500	9100	500	500
U-236	800	800	35	1600	800	800
U-238	800	800	35	1600	800	800
Th-234	3200	3200	3200	5800	3200	3200
U-234	35	800	35	1600	800	800

[a] Values from Reference 6 unless otherwise noted.
[b] Uranium soil K_d values from reference 8, assuming no organic material present.
[c] Soil K_d used for barrier and drain materials

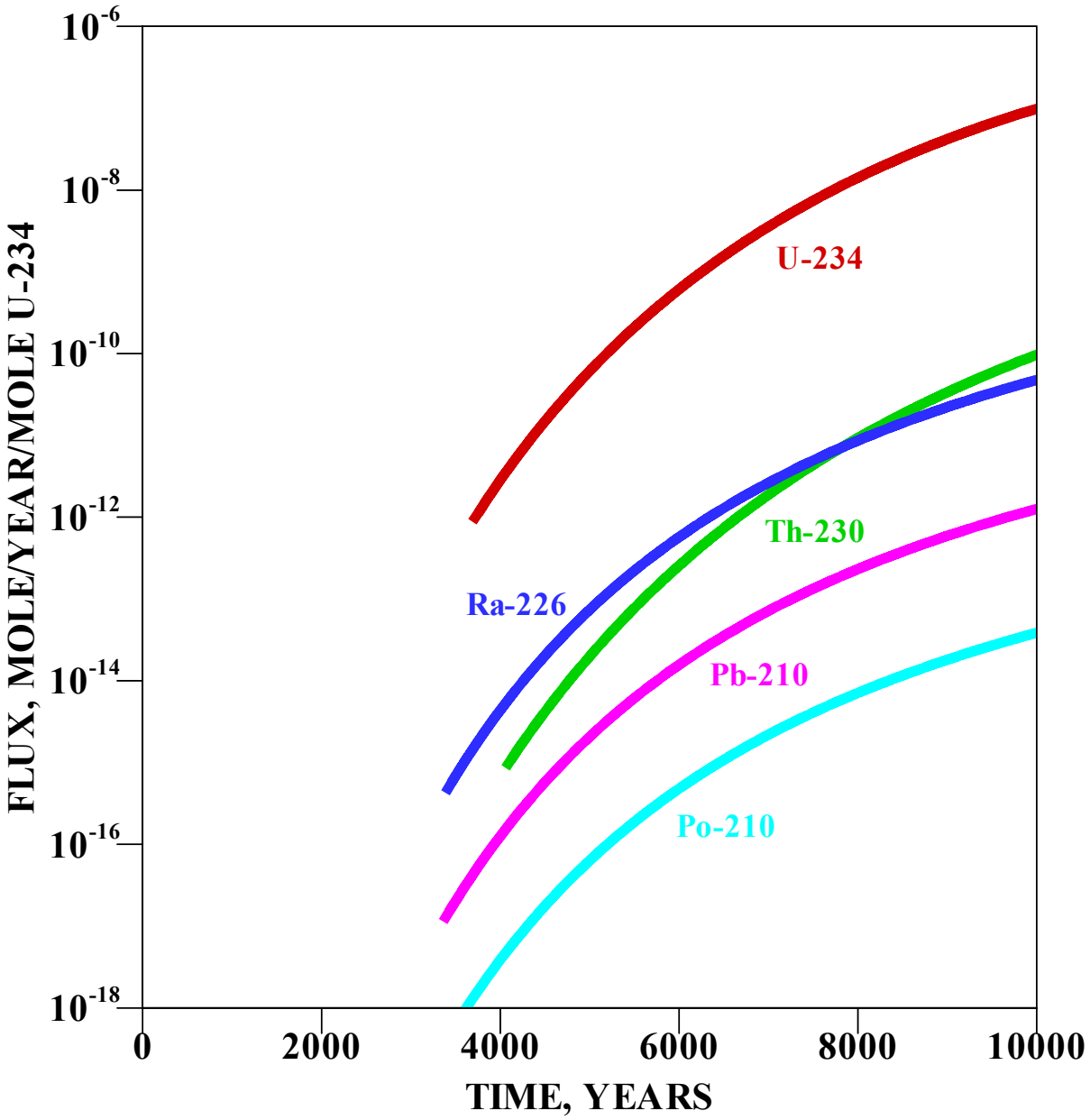

Figure 19. Instantaneous fluxes for U234 → Th-230 → Ra-226→ Pb-210 → Po-210.

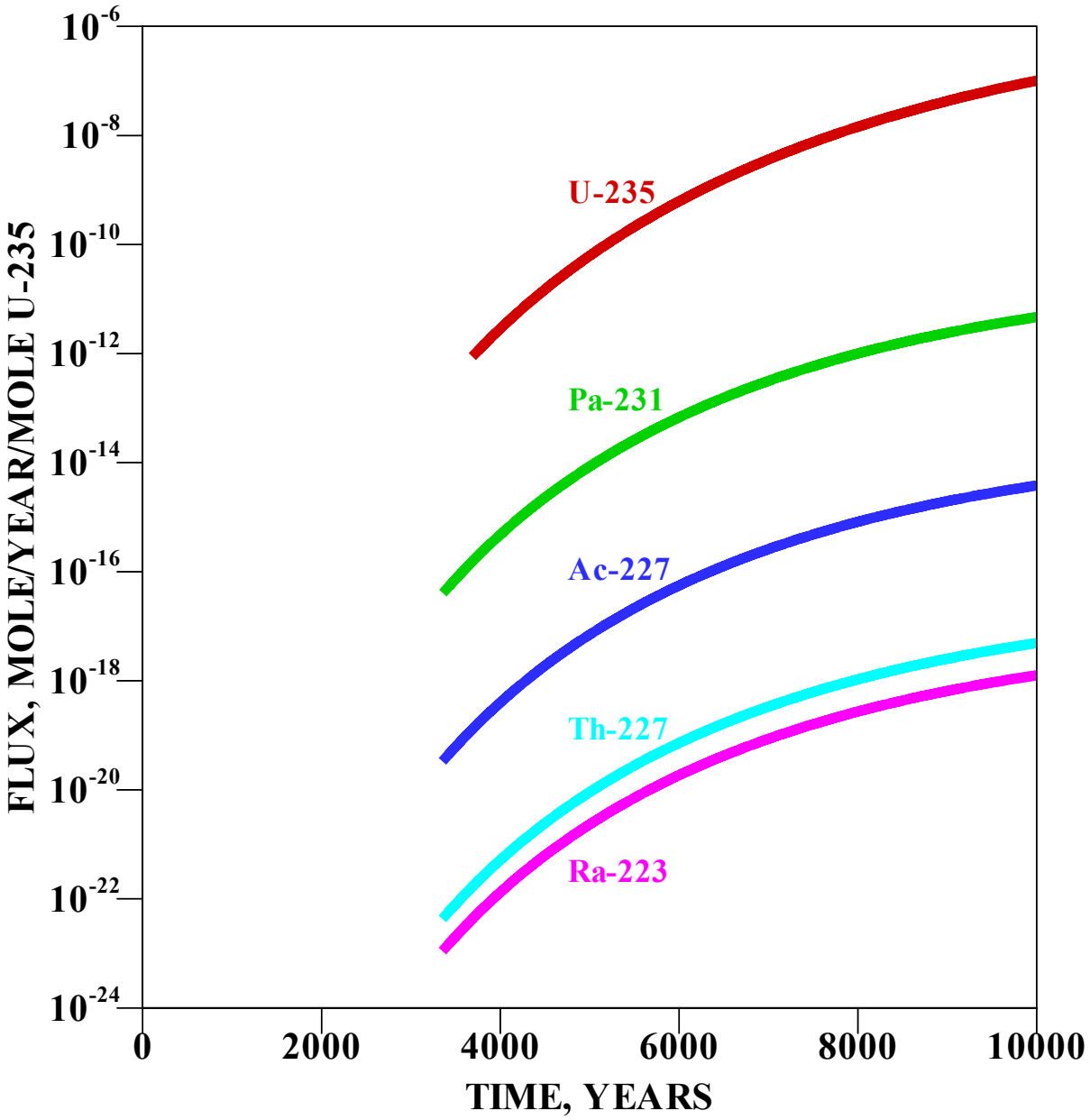

Figure 20. Instantaneous fluxes for U235 → Pa-231 → Ac-227→ Th-227 → Ra-223.

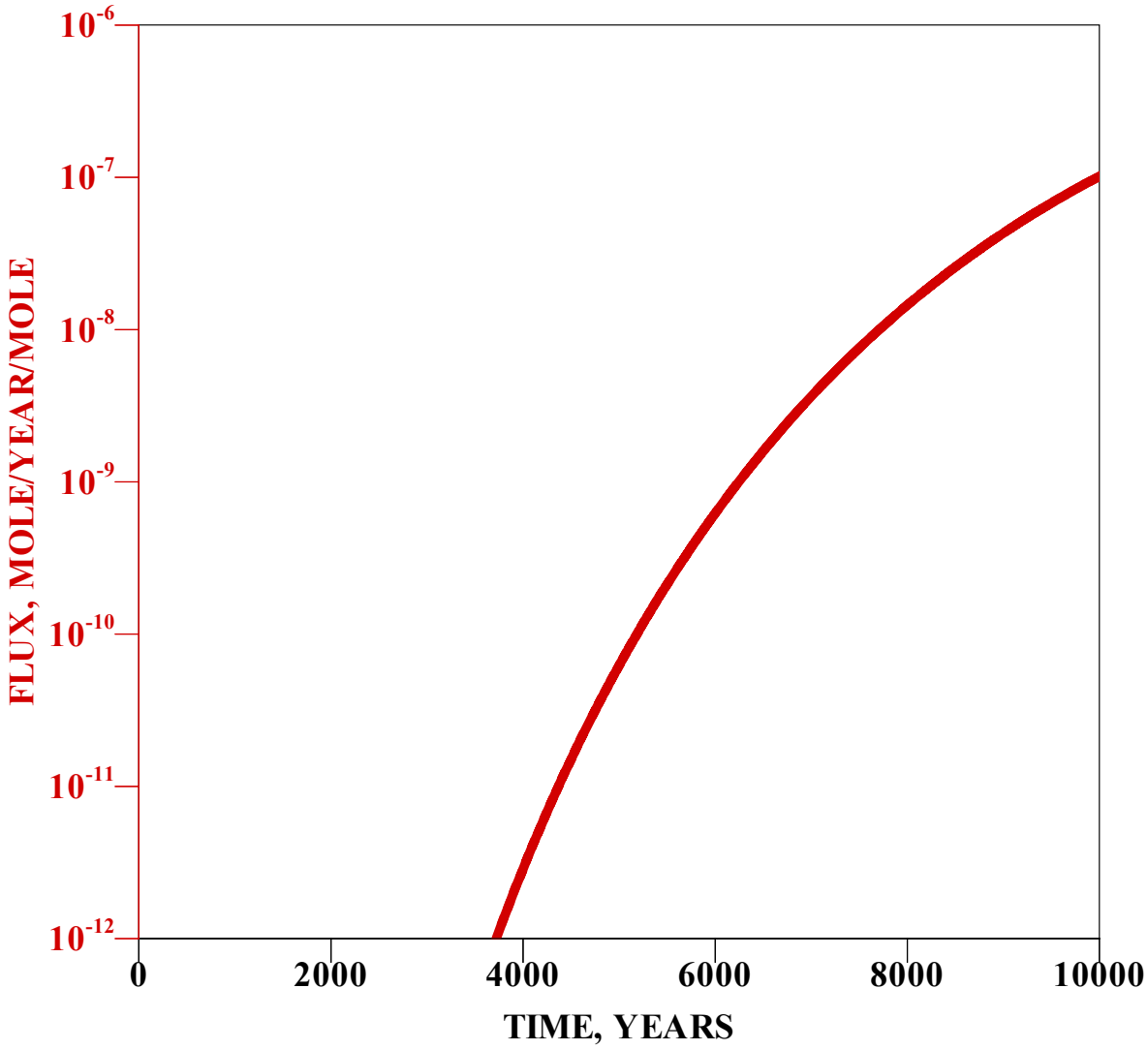

Figure 21. Instantaneous flux for U-236.

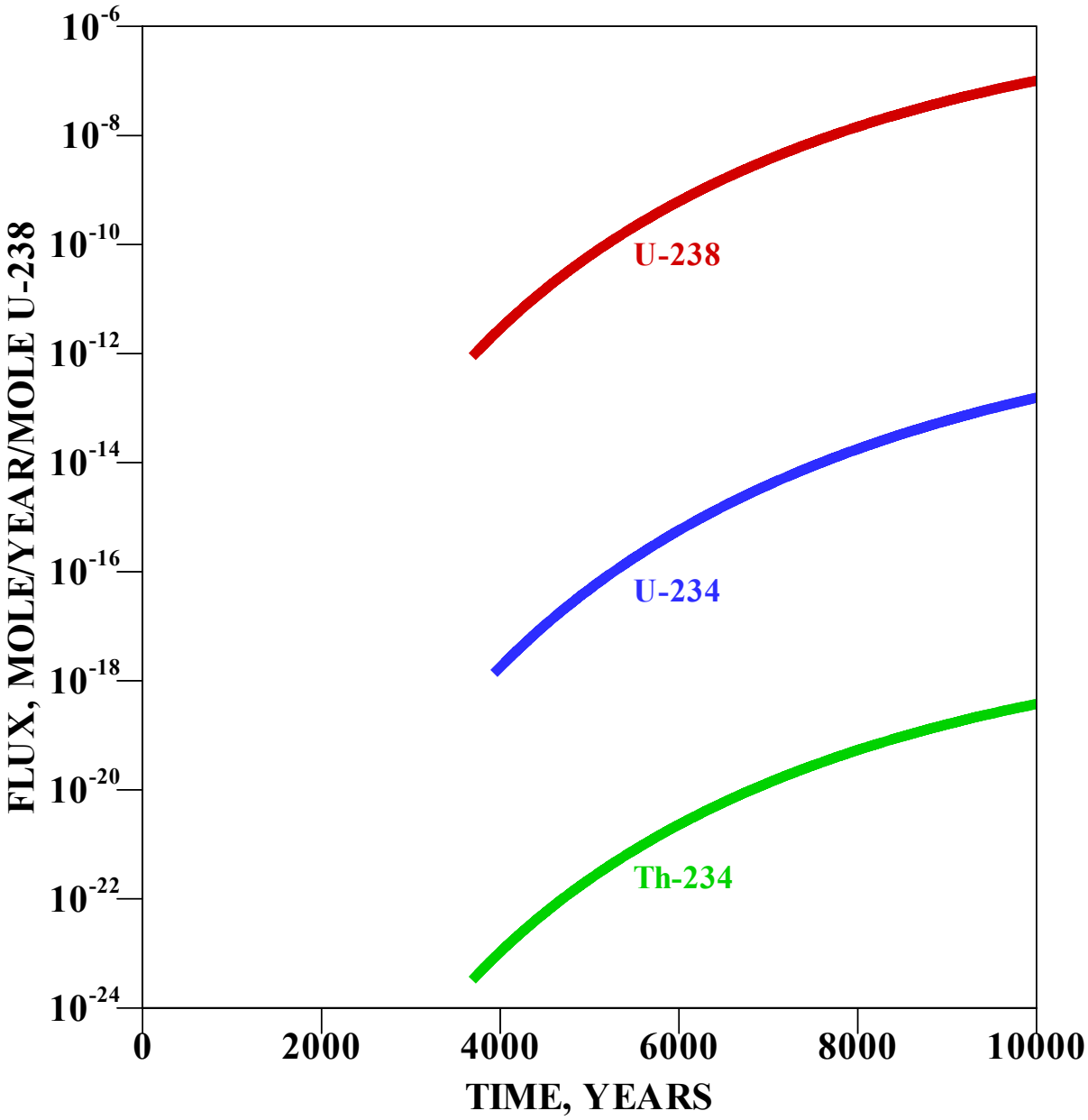

Figure 22. Instantaneous fluxes for U238 → Th-234 → U-234.

Table 7. Predicted peak flux and peak time for contaminant release to the water table.

Nuclides	Peak Flux Moles/yr/mole parent	Peak Time Years
U-234	1.19E-07	10,000
Th-230	1.16E-10	10,000
Ra-226	5.71E-11	10,000
Pb-210	1.51E-12	10,000
Po-210	4.63E-14	10,000
U-235	1.22E-07	10,000
Pa-231	5.60E-12	10,000
Ac-227	4.57E-15	10,000
Th-227	1.51E-18	10,000
Ra-223	5.90E-18	10,000
U-236	1.22E-07	10,000
U-238	1.22E-07	10,000
Th-234	4.50E-19	10,000
U-234	1.86E-13	10,000

[a] Based on the Design Check, these values were increased 20% over what is shown in Figures 19 through 22.

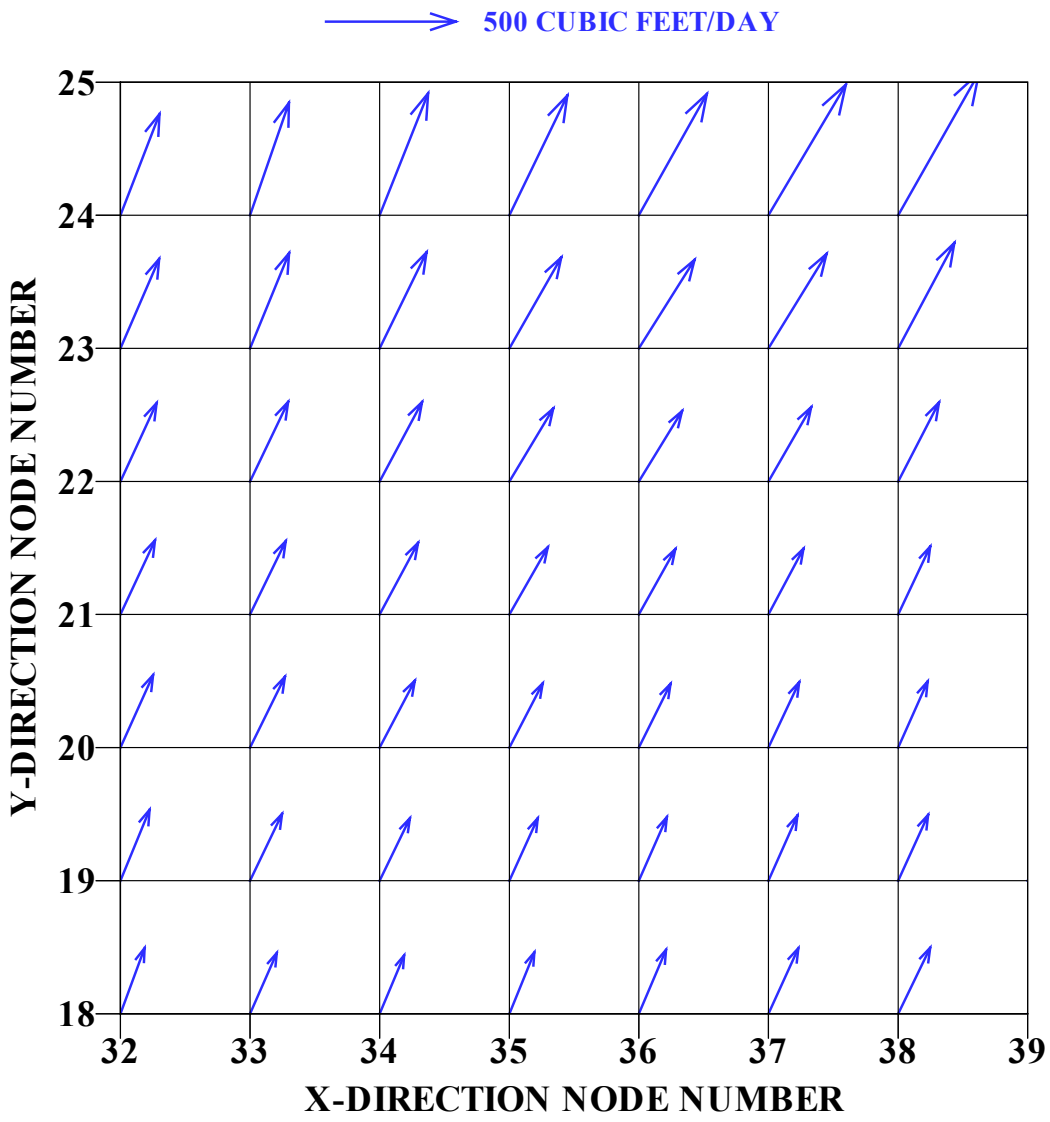

Figure 23. Volumetric flow rates in the vicinity of source nodes and compliance nodes. Horizontal slice, NZ=8

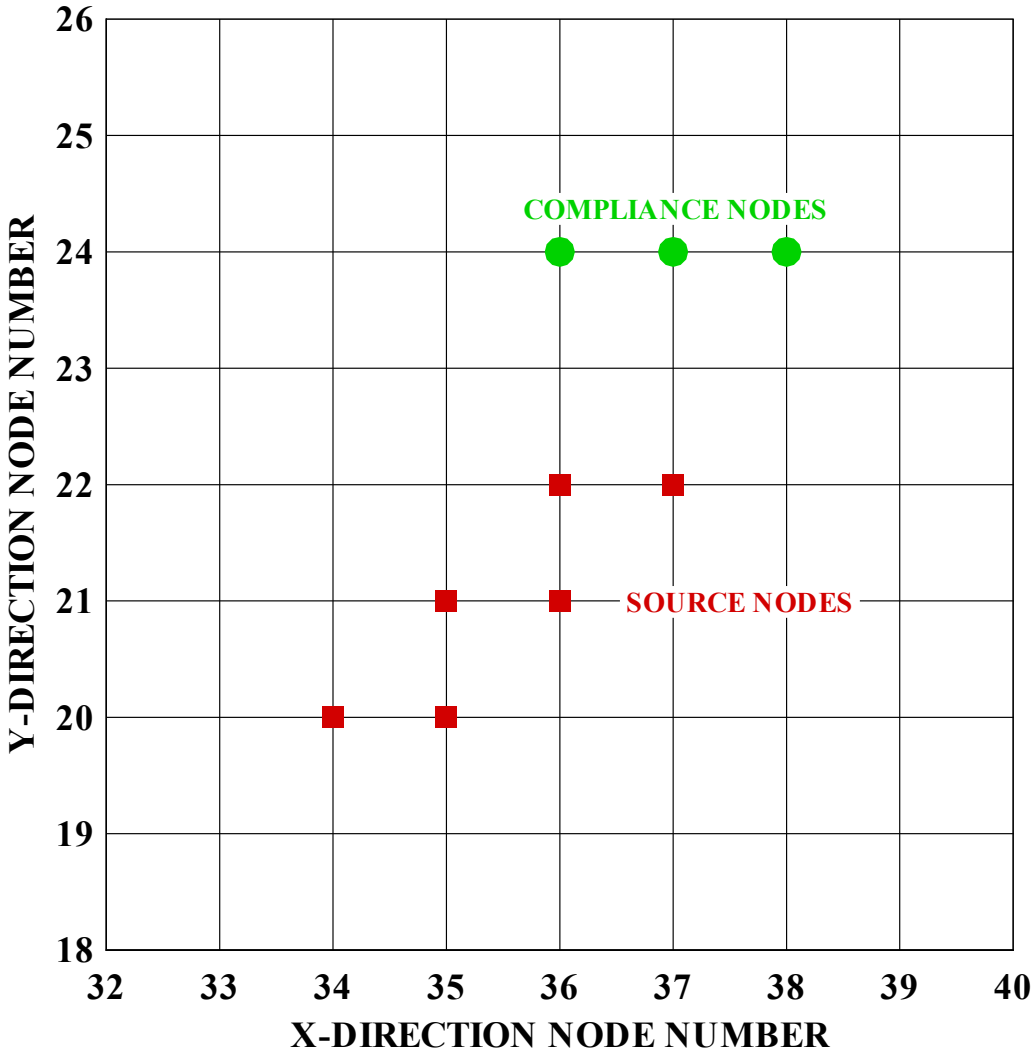

Figure 24. Location of the source and compliance nodes.

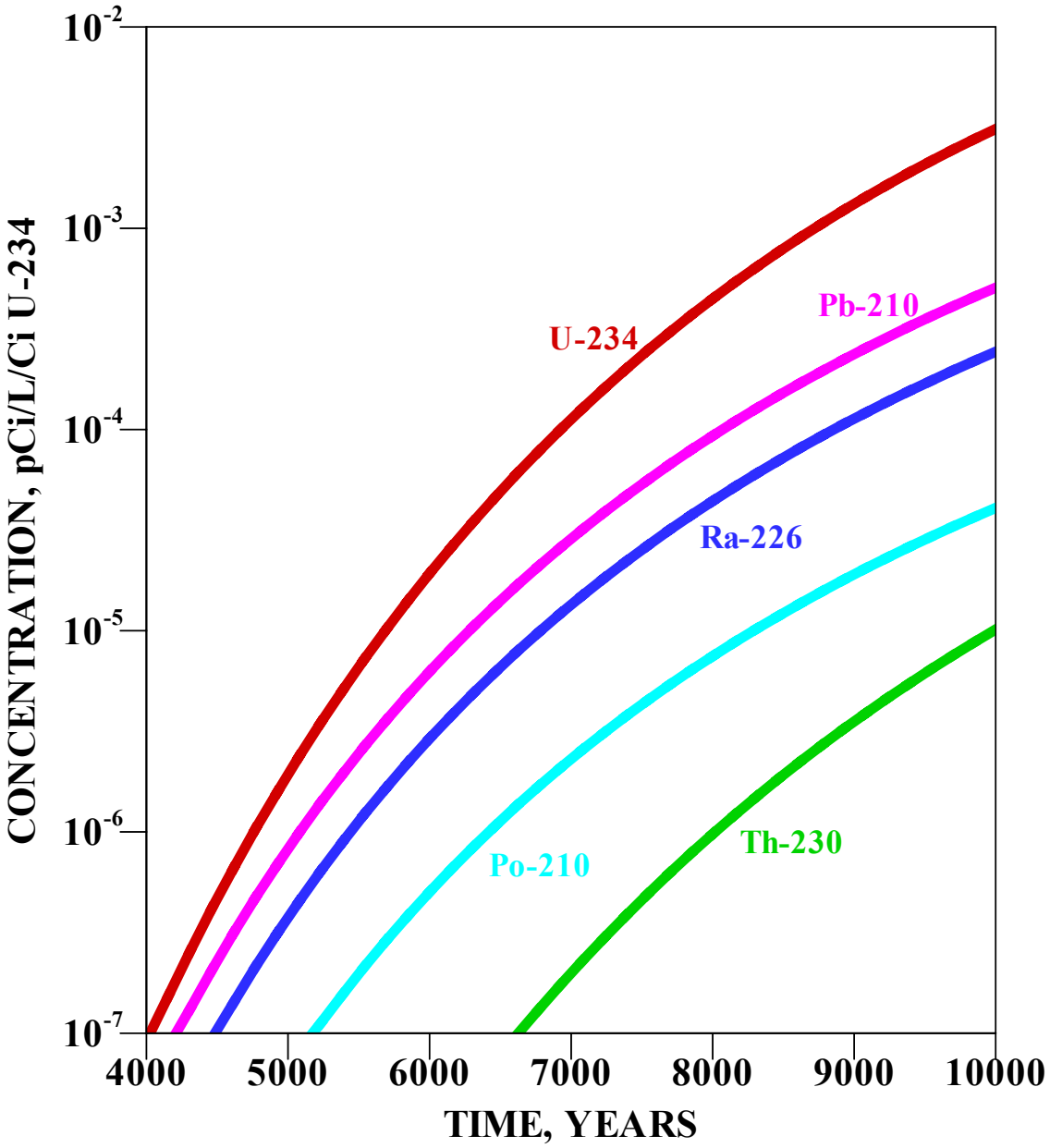

Figure 25. Concentration history at the peak node for U234 → Th-230 → Ra-226→ Pb-210 → Po-210.

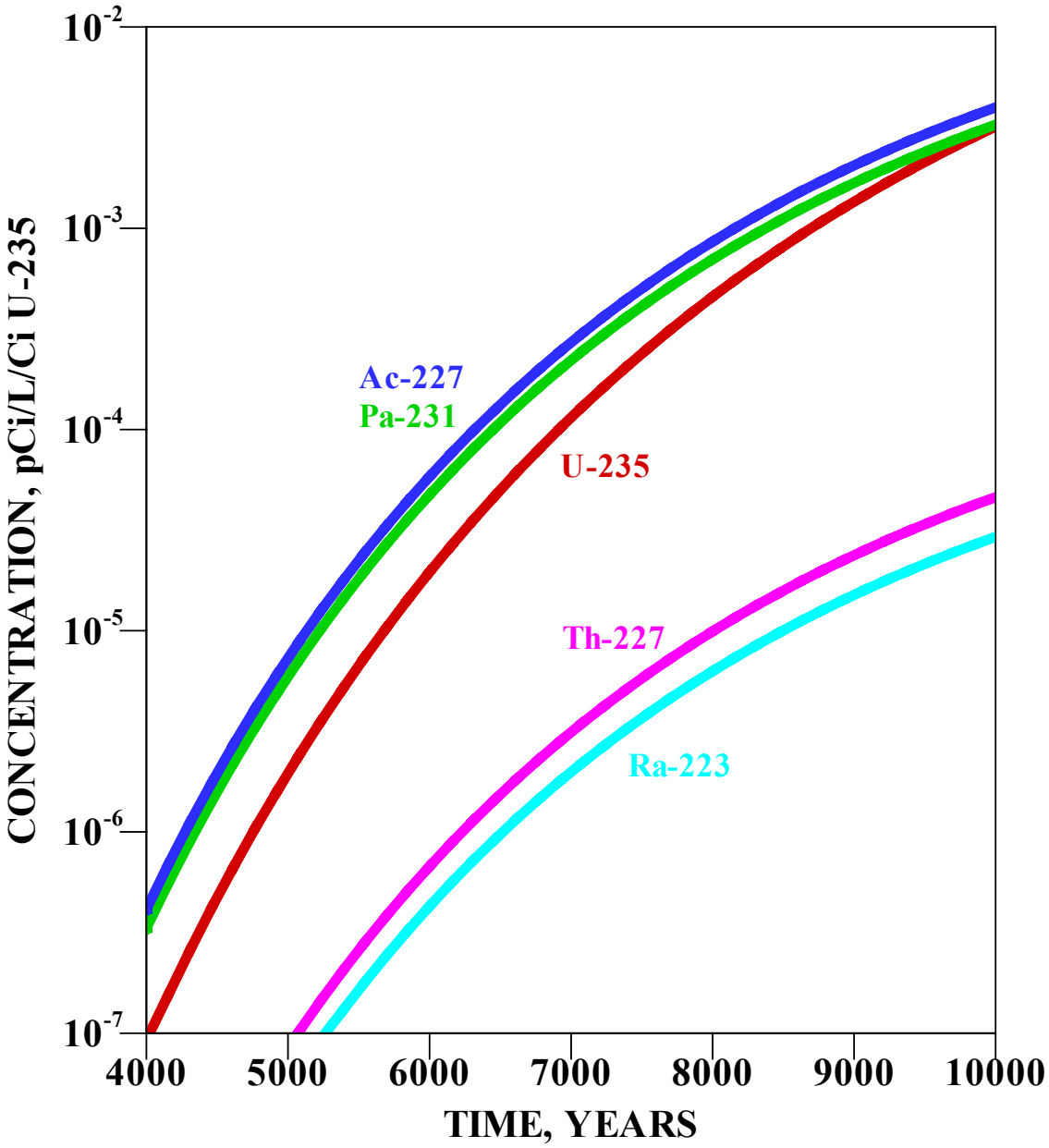

Figure 26. Concentration history at the peak node for U235 → Pa-231 → Ac-227→ Th-227 → Ra-223.

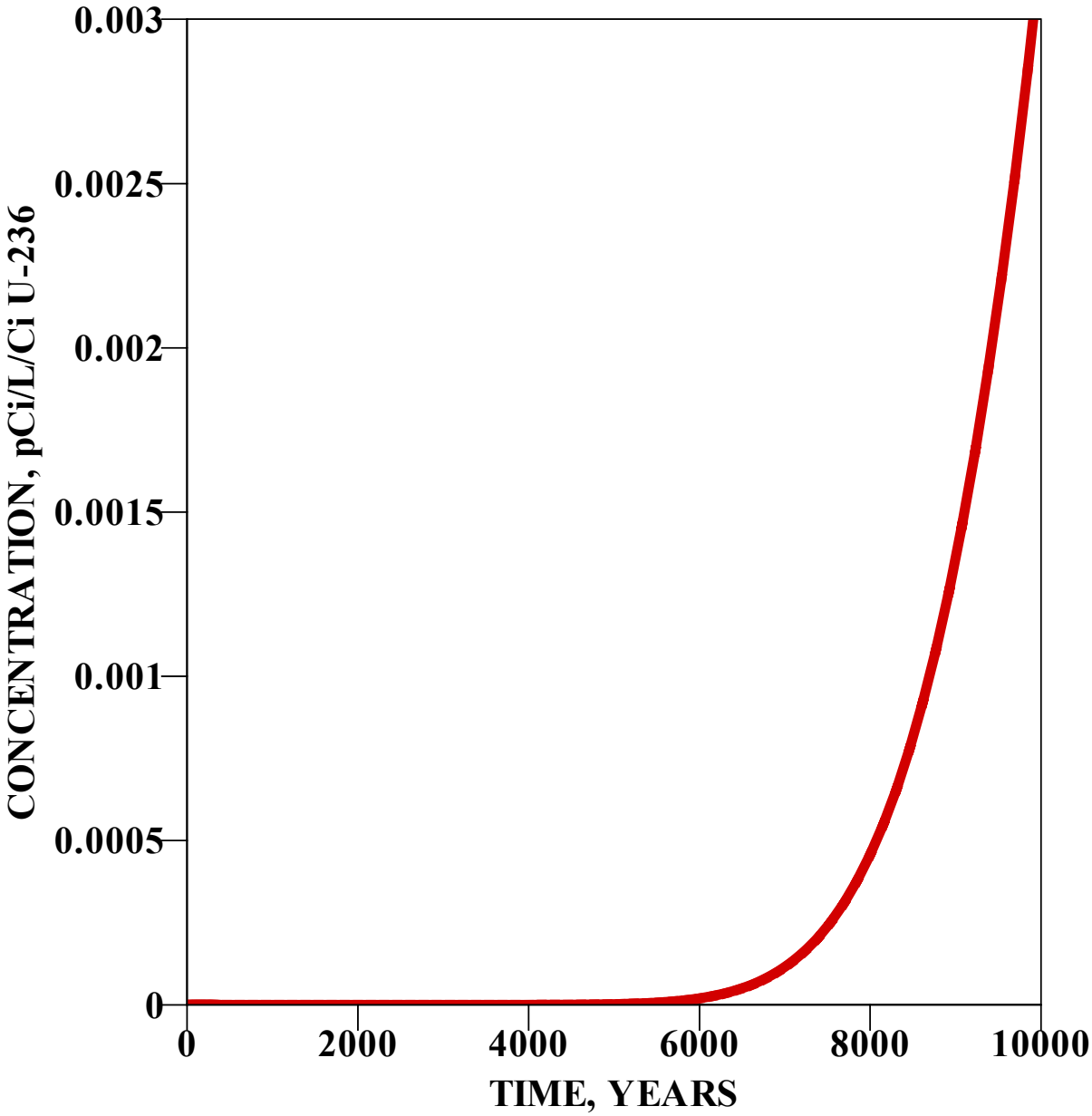

Figure 27. Concentration history at the peak node for U-236.

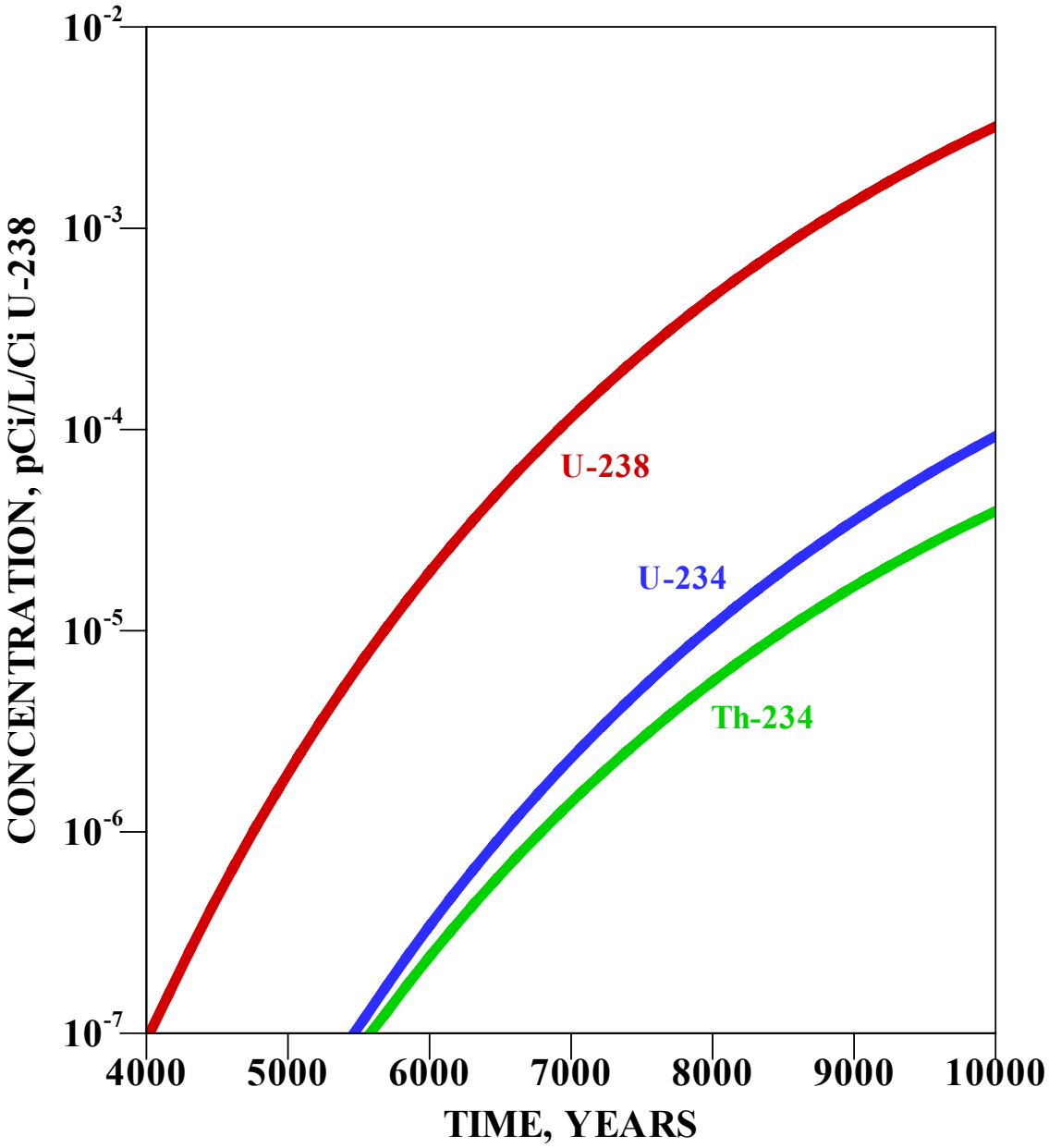

Figure 28. Concentration history at the peak node for U238 → Th-234 → U-234.

Figure 29 shows the U-238 concentrations at 10,000 years in the vertical plane containing all compliance nodes. A maximum concentration of 3.2E-03 pCi/L/Ci is predicted at node (37,24,8). The distribution of U-238 in the horizontal plane at 10,000 years is shown in Figure 30.

Table 8 lists the predicted peak groundwater concentration, peak time, and peak node for each of the species considered in the study. The node at which the peak concentration occurs is the same for each of the species. Table 9 compares the peak concentrations found in this study with those in PA Revision 1. In all cases the peak concentrations were lower.

Table 10 lists the predicted peak concentration, maximum concentration limit (MCL) and calculated inventory limits for each uranium isotope. Table 11 compares the calculated inventory limits and the measured inventory for the uranium isotopes. This table shows that the inventory is more than 100 times lower than the calculated limits.

INTRUDER CONSIDERATIONS

Since the vitrified waste form of the M-Area Glass retains uranium to a much greater extent than was analyzed in the Performance Assessment, the potential for decreased intruder-based limits due reduced leaching of radionuclides from the waste does exist. To assess this situation, the intruder analysis for trench disposal of the uranium isotopes was reevaluated.

The nature of the vitrified waste form makes two fundamental changes in the intruder analysis. The first is that the waste product will be recognizable as something different than native soil for a very long time. Figure 4 shows that after 10,000 years only 2.5% of the mass of each glass piece will have been removed. The excavation part of the agriculture scenario would bring a large quantity of the glass material to the surface. The Implementation Guide for DOE Order 435.1[9] states "Intruder scenarios need to consider the following: … An intruder will usually take reasonable, investigative actions upon discovery of unusual materials…" The glass waste form is sufficiently different from soil at SRS, that it would be investigated and the excavation stopped. Therefore, the agricultural scenario has been removed from consideration in this analysis.

The Post-Drilling and Resident scenarios for trench disposal were recalculated without leaching. The results are given in Table 12.

RADON PATHWAY

The limit for U-234 disposal in trench disposal units due to radon generation is 49 Ci/5 trenches[6]. This is significantly higher than the inventory of 2.8 curies in the M-Area Glass.

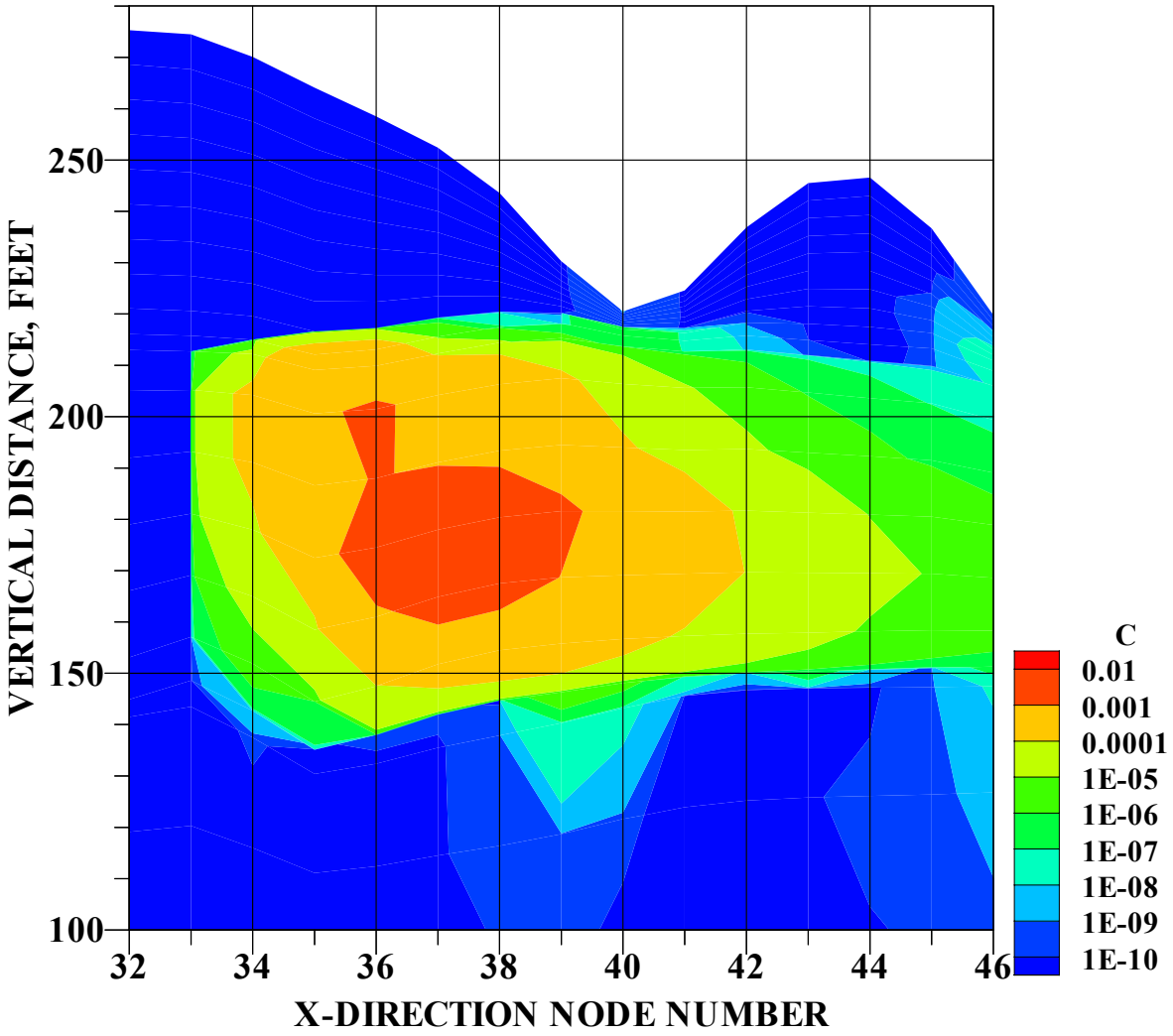

Figure 29. Plume of U-238 at 10,000 years in the vertical plane containing compliance points.

This figure depicts the U-238 concentrations at 10,000 years in the vertical plane containing all compliance nodes. A maximum concentration of 3.2E-03 pCi/L/Ci is predicted at node (37,24,8). Note that the vertical scale is in feet and the horizontal scale is by node number. The nodes are 200 feet apart.

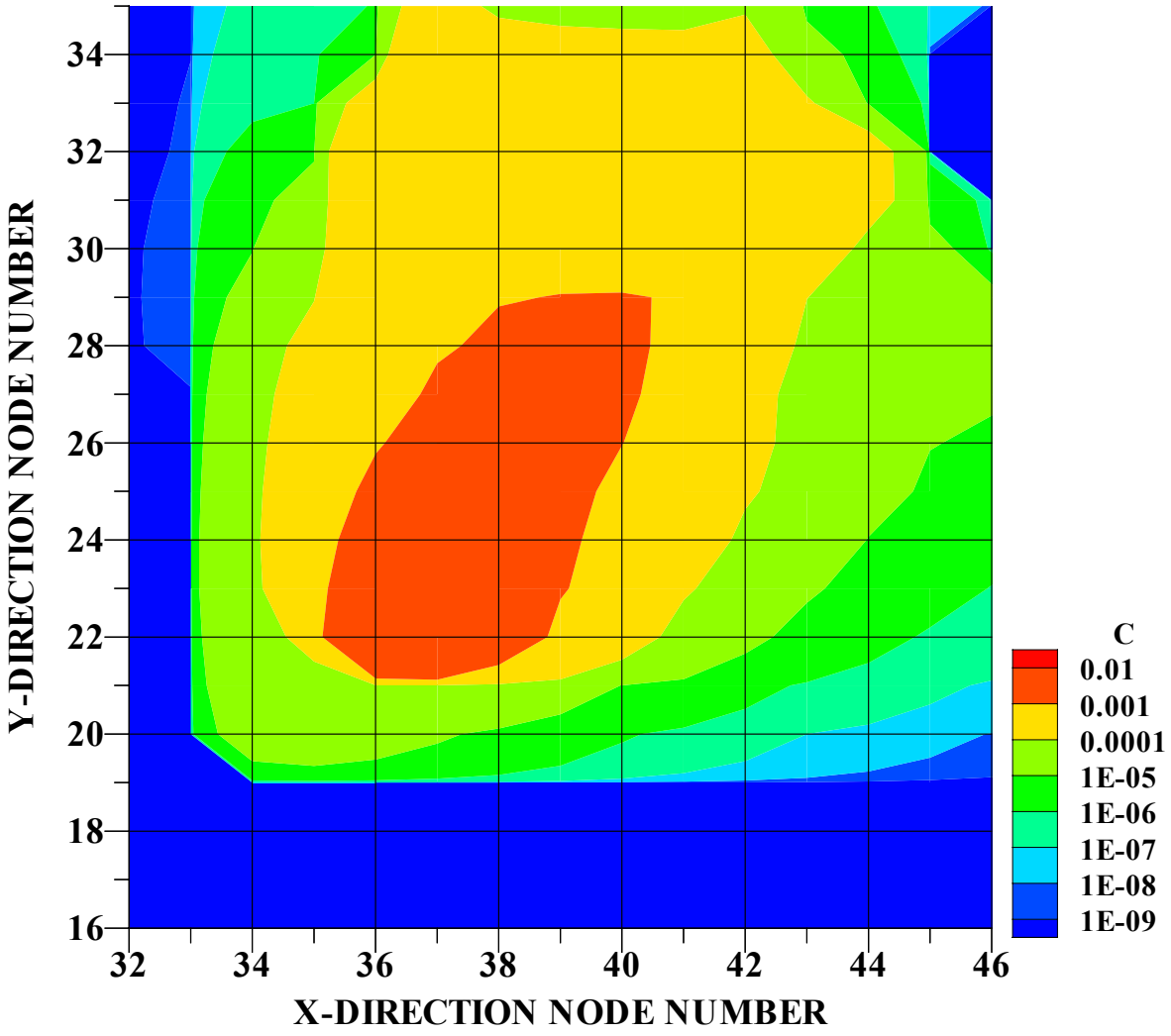

Figure 30. Plume of U-238 at 10,000 years in the horizontal plane containing the peak node.

This figure depicts the U-238 concentrations at 10,000 years in a "horizontal" plane containing the peak node. Data selected are NZ=8 and may vary slightly in elevation. A maximum concentration of 3.2E-03 pCi/L/Ci is predicted at node (37,24,8). This figure contains two of the source nodes [(36,22,8) and (37,22,8)] where the concentrations are higher than the peak node.

Table 8. Predicted peak groundwater concentration, peak time, and peak node based on 1.0 mole of parent component.

Nuclides	Peak Concentration pico-moles/L/mole[a]	Peak Time Years	Peak Node*
U-234	3.74E-03	10,000	37,24,8
Th-230	3.70E-06	10,000	37,24,8
Ra-226	1.80E-06	10,000	37,24,8
Pb-210	4.46E-08	10,000	37,24,8
Po-210	6.10E-11	10,000	37,24,8
U-235	3.85E-03	10,000	37,24,8
Pa-231	1.48E-07	10,000	37,24,8
Ac-227	1.38E-10	10,000	37,24,8
Th-227	3.77E-15	10,000	37,24,8
Ra-223	1.40E-15	10,000	37,24,8
U-236	3.85E-03	10,000	37,24,8
U-238	3.85E-03	10,000	37,24,8
Th-234	6.73E-16	10,000	37,24,8
U-234	5.89E-09	10,000	37,24,8

Table 9. Comparison of peak concentration and peak time between this study and PA Rev. 1 based on 1.0 Ci of parent component.

	This Study		PA Rev. 1.	
	Peak Conc.	Peak Time*	Peak Conc.	Peak Time
Nuclides	pCi/L/Ci	Years	pCi/L/Ci	Years
U-234	3.74E-03	10,000	1.39E+01	1,170
Th-230	1.21E-05	10,000	4.22E-03	7,290
Ra-226	2.93E-04	10,000	2.39E-02	14,200
Pb-210	6.08E-04	10,000	4.41E-02	14,200
Po-210	4.90E-05	10,000	7.94E-02	14,200
U-235	3.85E-03	10,000	1.40E+01	1,170
Pa-231	3.92E-03	10,000	5.11E-02	8,300
Ac-227	4.79E-03	10,000	6.27E-02	8,320
Th-227	5.53E-05	10,000	8.82E-03	8,320
Ra-223	3.52E-05	10,000	5.64E-02	8,320
U-236	3.85E-03	10,000	7.21E+02	5,880
U-238	3.85E-03	10,000	1.41E+01	1,170
Th-234	4.72E-05	10,000	1.54E-01	1,170
U-234	1.11E-04	10,000	4.88E-02	1,320

* Peak time after 10,000 years was not calculated. When peak time > 10,000 years, the concentration at 10,000 years is peak concentration shown.

Table 10. Predicted peak concentration, maximum concentration limit (MCL) and calculated inventory limit.

	Peak Concentration	MCL	Inventory Limit	Projected M-Area Waste Inventory
Nuclides	pCi/L/Ci	pCi/L	Ci/5 trenches	Ci
U-234	3.7E-03	1.3E+02	1.8E+04	2.8
Th-230	1.2E-05	1.5E+01	6.2E+05	
Ra-226	2.9E-04	5.0E+00	8.6E+03	
Pb-210	6.1E-04	1.0E+00	**8.2E+02**	
Po-210	4.9E-05	1.5E+01	1.5E+05	
U-235	3.8E-03	6.5E+01	8.6E+03	0.19
Pa-231	3.9E-03	3.1E+00	4.0E+02	
Ac-227	4.8E-03	1.0E+00	**1.0E+02**	
Th-227	5.5E-05	1.5E+01	1.4E+05	
Ra-223	3.5E-05	1.5E+01	2.1E+05	
U-236	3.8E-03	1.4E+02	**1.8E+04**	0.14
U-238	3.8E-03	1.0E+01	**1.3E+03**	11
Th-234	4.7E-05	4.0E+02	4.3E+06	
U-234	1.1E-04	1.3E+02	5.9E+05	

Table 11. Comparison of the calculated groundwater-based inventory limits for five Slit Trenches or one Engineered Trench and the projected inventory.			
	Inventory Limit,	Actual Inventory	Limit/Actual Inventory
Radionuclide	Ci/5 trenches	Ci	
U-234	8.2E+02	2.8E+00	2.9E+02
U-235	1.0E+02	1.9E-01	5.3E+02
U-236	1.8E+04	1.4E-01	1.3E+05
U-238	1.3E+03	1.1E+01	1.2E+02

Table 12. Intruder limits with no leaching versus M-Area Glass Inventory			
Radionuclide	Resident Limit, Ci	Post-Drilling Limit, Ci	M-Area Glass Inventory, Ci
U-234	4.3E+04	4.4E+03	2.8E+00
U-235	3.7E+01	3.9E+03	1.9E-01
U-236	1.3E+05	4.6E+03	1.4E-01
U-238	2.0E+02	4.8E+03	1.1E+01

DISPOSAL LIMITS

Disposal limits for disposal of the M-Area Glass waste form in either slit trenches or Engineered Trenches are shown in Table 13. The lowest of the limits calculated for the groundwater, resident and post-drilling scenarios is the one that should be used, and is given in bold type.

Table 13. Disposal Limits (Ci per 5 trenches or 1 Engineered Trench) for M-Area Glass					
Radionuclide	Radon Limit, Ci	Resident Limit, Ci	Post-Drilling Limit, Ci	Groundwater Limit, Ci	M-Area Glass Inventory, Ci
U-234	**4.9E+01**	4.3E+04	4.4E+03	8.2E+02	2.8E+00
U-235	**---**	**3.7E+01**	3.9E+03	1.0E+02	1.9E-01
U-236	---	1.3E+05	**4.6E+03**	1.8E+04	1.4E-01
U-238	**---**	**2.0E+02**	4.8E+03	1.3E+03	1.1E+01

Note: Most limiting pathway is shown in bold type.

CONCLUSIONS

This Special Analysis demonstrates that when the reduced release rate provided by the vitrified waste form is included in the analysis, the M-Area glass can be disposed in trench disposal units in E-Area. The analysis did not evaluate the effect of wood products interacting with the glass, therefore, no wood products should be disposed in the vicinity of the M Area Glass. It is well

known that glass is more soluble in a high pH environment, so the M Area Glass should not be disposed near any wastes containing cement-based products.

The Composite Analysis showed that there would be very little effect to offsite individuals from E-Area. This study shows that the disposal of M-Area glass will meet the performance objective for low-level waste disposal, so the conclusion of the Composite Analysis[10] will not change.

Subsequent to the modeling work described in this report, data on the actual M-Area waste glass became available. The glass type used was the one with the lowest dissolution rate of those shown in Table 2. Appendix A uses the actual glass information to demonstrate that the analysis in the Special Analysis is conservative.

QUALITY ASSURANCE

The report underwent a design check which is documented in Reference 11. The design check was intended to conform to the guidelines in Reference 12.

REFERENCES

1. Federal Register: March 15, 2002, Volume 67, Number 51.

2. Federal Register: August 21, 2002, Volume 67, Number 162.

3. *Categorical Exclusion Unreviewed Safety Question*, USQ-SWE-2001-0049, Sequence Number 1629, Shawn R. Reed, 1/15/2002.

4. *Special Analysis: Correction and Update of E-Area Disposal Limits*, WSRC-TR-2002-00047, Revision 2, Savannah River Technology Center, May 2, 2002., Rev. 6, August 1, 2001.

5. A. Ryan Whited, A. Ryan, Robert A. Fjeld and James R. Cook, *Vitrified Waste Form Performance Modeling Applied to the Treatment and Disposal of a Mixed-Waste Sludge at the Savannah River Site*, Nuclear Technology, Vol. 123, pp. 304-319, Sep. 1998.

6. *Radiological Performance Assessment for the E-Area Vaults Disposal Facility.* WSRC-RP-94-218, Rev. 1. Savannah River Technology Center, Westinghouse Savannah River Company, Aiken, SC., January 31, 2000.

7. ACRI. *PORFLOW: A Model for Fluid Flow, Heat and Mass Transport in Multifluid, Multiphase Fractured or Porous Media, Users Manual, Version 3.0*. Draft. Analytic and Computational Research, Inc., Los Angeles, CA (1996).

8. *Uranium Geochemistry in Soil and Groundwater at the F and H Seepage Basins*, EPD-SGS-94-307, Rev. 0, Westinghouse Savannah River Company, Aiken, SC September 1994.

9. *Implementation Guide for use with DOE M 435.1-1, Chapter IV, Low Level Waste Requirements*, DOE G 435.1-1, July 9, 1999.

10. *Composite Analysis E-Area Vaults and Saltstone Disposal Facilities,* WSRC-RP-97-311, Rev. 0, Savannah River Technology Center, Westinghouse Savannah River Company, Aiken, SC September 1997.

11. *Design Check Package for Special Analysis: Disposal of M-Area Glass in Trenches*, WSRC-TR-2002-00xx, August 13, 2002.

12. *Technical Report Design Check Guidelines*, WSRC-IM-2002-00011, August 12, 2002.

THIS PAGE INTENTIONALLY LEFT BLANK

APPENDIX A

SUPPLEMENTAL INFORMATION

THIS PAGE INTENTIONALLY LEFT BLANK

APPENDIX A

After the calculations for the performance assessment were completed, data on the actual M-Area glass waste form became available. This Appendix was prepared to compare the PA wasteform assumptions and the actual data and evaluate the effect this would have had on the results presented in the SA.

Physical Dimensions and Dissolution Rate

As shown in Figure A-1, the glass material is greatly flattened. The SA characterized the leaching properties of a hemisphere, while the photograph indicates a disk might be more appropriate. The typical dimensions of the beads were given by Pickett[1] to be one-half inch in diameter and one-quarter in on thickness. The surface area of a cylinder is the area of the top and bottom circular surfaces ($2\pi r^2$) plus the circumference of the circle times the height ($2\pi rh$). The radius and the height are both one-quarter of an inch, or 2.54 cm/in*0.25 = 0.635 cm

The surface area-leachate volume ratio for this would then be:

$$2*\pi*(0.635)^2 + 2*\pi*0.635*0.635\backslash 10\ cm^3 = 0.51\ cm^{-1} \text{ or } 51\ m^{-1}.$$

Pickett[1] stated that the M-area glass was of the SRL-165 variety. Table 2 in the SA gives the long-tern dissolution rate for SRL-165 glass at two SA/V values. The value of 51 m^{-1} falls outside the range for the SRL-165 data in the table. The data indicate that SRL-165 dissolution decreases slightly with decreasing SA/V. Applying the Arrhenius temperature dependence equation to the k value for the SA/V of 340 gives a dissolution rate at 25°C of 1.0E-6 $g/m^2/d$. This is more than an order of magnitude lower than the initial dissolution rate of 2.5E-5 $g/m^2/d$ used in the SA. The SA thus is quite conservative in the groundwater pathway calculations.

Effect of "Strings" of Glass

Figure A-1 shows a portion of the glass has formed into "strings." As the drums corrode and things settle, it is credible that this portion of the material will form a fine powder, which could leach uranium at a higher rate than the bulk of the glass.

Reference 2 derives a formula for the change in radius of a spherical glass particle as a function of the leach rate and glass density as:

$$\frac{dR(t)}{dt} = -\frac{LR}{\rho}$$

Using the higher SA/V dissolution rate for SRL-165 glass from Table 2 of 3.1E-4 $g/m^2/d$ and the Arrhenius temperature correction factor of 0.0044 from the SA, gives a dissolution rate at 25° C of 1.4E-06 $g/m^2/d$, or 5.0E-04 $g/m^2/yr$. Using this rate and a glass density of 2.6E06 g/m^3 in the

Figure A-1. M-Area waste glass in disposal drum.

above equation gives a rate of radius change per year of 1.9E-10 m/y. If we assume that the strings break up into particles with a radius of 0.05 mm (the approximate size of the ground glass used in the leaching tests), then the time for each to dissolve is:

5E-5 m/1.9E-10 m/yr = 2.6E5 years

The inverse of this is the annual leach rate, 3.8E-6 yr^{-1}.

For comparison, the current trench disposal limits for uranium are based on a uranium K_d of 4 ml/g in the waste zone, an infiltration rate of 40 cm/yr, a waste thickness of 4.6 m, a density of 1.5 g/cm^3 and a waste porosity of 0.42. Using the equation from Baes and Sharp[3],

$$FLR = \frac{I/\Theta}{d(1+\frac{\rho K_d}{\Theta})}$$

where,

FLR = Fractional leach rate, yr^{-1}

I = Infiltration rate, cm/yr

Θ = porosity

d = waste thickness, cm

ρ = density, g/cm^3

K_d = partition coefficient, cm^3/g,

gives a leach rate of 1.4E-2 yr^{-1}.

Comparison of the small glass particle leach rate with the normal waste leach rate show that the glass will release uranium about 3700 times more slowly. All other factors being the same, the trench disposal limit for the "strings" would be 3700 times greater than the trench disposal limit for normal uranium waste. Pickett[1] estimated the volume percentage, and therefore the inventory percentage, of the "strings" at 2 to 5 percent. The effect of this on the groundwater pathway results can be estimated by comparing 5 percent of the M-Area waste inventory to 3700 times the trench limits for unenhanced waste form disposal.[4] This comparison is given in Table A-1.

Table A-1 Comparison of maximum "string" inventory with estimated trench inventory limits

Radionuclide	Inventory, Ci	"String" Inventory, Ci	Estimated Trench Limit for Glass "Strings", Ci	Inventory/Limit
U-234	2.8E+00	1.4E-01	4.1E+04	4.8E-06
U-235	1.9E-01	9.5E-03	3.0E+04	7.3E-07
U-236	1.4E-01	7.0E-03	7.4E+03	1.3E-06
U-238	1.1E+01	5.5E-01	2.7E+04	2.9E-05

Table A-1 shows that a conservative high-side estimate of the inventory contained in the “strings” is many orders of magnitude below the allowable limits. The presence of the ”strings” in the disposal drums has so little impact on the groundwater pathway that they need not be considered further. Therefore, the limits shown in Table 13, based on the intruder analysis and radon emanation rates, should be applied to the disposal of M-Area Glass.

References

1. John Pickett, Personal Communication, August 15, 2002.

2. Whited, Aaron Ryan, *Vitrified Waste Form Performance Modeling Applied to the Disposal of a Mixed Waste Sludge at the Savannah River Site*, Masters Thesis, Clemson University, August 1996.

3. Baes, C. F., III and Sharp, R. D., *A Proposal for Estimation of Soil Leaching Constants for Use in Assessment Models*, Journal of Environmental Quality, vol. 12, no. 1, pp. 17-28, 1983.

4. *Special Analysis: Correction and Update of E-Area Disposal Limits*, WSRC-TR-2002-00047, Revision 1, March 15, 2002.